Mathematisches Forschungsinstitut Oberwolfach

Report No. 49/2018

DOI: 10.4171/OWR/2018/49

Emergence of Structures in Particle Systems: Mechanics, Analysis and Computation

Organised by
Andrea Braides, Rome
Bernd Schmidt, Augsburg
Ulisse Stefanelli, Vienna
Florian Theil, Warwick

28 October – 3 November 2018

Abstract. The meeting focused on the last advances in particle systems. The talks covered a broad range of topics, ranging from questions in crystallization and atomistic systems to mesoscopic models of defects to machine learning approaches and computational aspects.

Mathematics Subject Classification (2010): 49x, 74x, 82Dx.

Introduction by the Organisers

Let us start by Richard Feynman's famous quote on the atomistic hypothesis from his Lectures on Physics (vol. 1, chapter 1):

> *If, in some cataclysm, all of scientific knowledge were to be destroyed, and only one sentence passed on to the next generations of creatures, what statement would contain the most information in the fewest words? I believe it is the atomic hypothesis (or the atomic fact, or whatever you wish to call it) that all things are made of atoms–little particles that move around in perpetual motion, attracting each other when they are a little distance apart, but repelling upon being squeezed into one another. In that one sentence, you will see, there is an enormous amount of information about the world, if just a little imagination and thinking are applied.*

Understanding the macroscopic behavior of matter from fundamental principles is indeed among the most fascinating open challenges in Materials Science. Here,

one is interested in the study of particle systems driven by quantum mechanical interaction potentials. The precise description of large particle systems geometry is presently still eluding a comprehensive mathematical discussion. The emergence of large structures such as crystals, patterns, interfaces, and Wulff shapes as well as in the quantification of defects and surface instability effects are presently attracting significant attention.

The micro-mechanics of particle systems has to be addressed in order to describe elastic response, especially across scales, the emergence of mesoscopic microstructures such as fractures or grain boundaries, and the dynamics of dislocations and defects. By increasing the size of the system one is then interested in the passage to continua where, possibly, mesoscopic length or timescales arise.

A thorough and comprehensive understanding of such diverse phenomena will eventually have to be approached from different angles and hinge on combined efforts: Starting from first principles considerations and classical point mechanics, methods from statistical physics as well as variational techniques will have to be employed, modeling issues need to be addressed at various mesoscales, and efficient numerical schemes are to be developed at large scales resolving atomistic defects.

The workshop, organized by Andrea Braides (Roma), Bernd Schmidt (Augsburg), Ulisse Stefanelli (Vienna), and Florian Theil (Warwick), aimed at presenting recent and promising achievements in this wide area. Over 50 participants with broad geographic representation and a variety of research fields intervened, each revealing different methodology, interests, and level of abstraction.

Among the many themes presented during the workshop, we record here

- Γ-convergence for crystalline models and for discretizations of free-discontinuity problems, also in presence of anisotropies.
- Optimal geometry of distributed masses on a Bravais lattice and particle numerical methods.
- Defects in crystals, stratified lower-dimensional crystalline structures, their mechanical and electronic properties.
- Variational problems for clustering on large graphs.
- Hyperuniformity and the phase transition between order and disorder in particle systems.
- Carbon nanostructures, nanotubes, and ripples in graphene.
- Collective behaviors in multiagents systems.
- Machine learning approaches to image reconstruction, empirical interatomic potentials, and large data clouds.

One of the organizers' main goal was to generate a strong interaction between various subjects and people working on different aspects of particle systems with different backgrounds. Approximately 25 talks were delivered by experts in the fields and post-docs and stimulated a lot of discussions in a friendly and inspiring atmosphere, that contributed to the overall success of the meeting. In particular, four participants (Carola-Bibiane Schönlieb, Charles Radin, Paolo Cermelli, Dejan Slepcev) contributed longer talks, broader in context, and hinting to many open issues.

Acknowledgement: The MFO and the workshop organizers would like to thank the National Science Foundation for supporting the participation of junior researchers in the workshop by the grant DMS-1641185, "US Junior Oberwolfach Fellows".

Workshop: Emergence of Structures in Particle Systems: Mechanics, Analysis and Computation

Table of Contents

Abstracts

Scaling limits and decay of correlations for non-convex energies

Stefan Adams

We study non-convex perturbations of the massless free Gaussian field (GFF) in dimensions $d = 2, 3$. We first show [2] the strict convexity of the surface tension for large enough β (low temperatures) and sufficiently small tilt, using multi-scale (renormalisation group theory) techniques based on a finite range decomposition of the underlying background Gaussian measure in [3].

Note also that, due to the gradient interaction, the Hamiltonian has a continuous symmetry. In particular this implies that no Gibbs measures on $\mathbb{Z}^d$ exist for dimensions $d = 1, 2$ where the field 'delocalises'. If one considers the corresponding random field of gradients (discrete gradient image of the height field φ) it is clear that its distribution depends on the gradient of the boundary condition of the height field. One can also introduce gradient Gibbs measures in terms of conditional distributions satisfying DLR equations. For strictly convex interaction W with bounds on the second derivative, Funaki and Spohn proved in 1997 the existence and uniqueness of an extremal, i.e. ergodic, gradient Gibbs measure for each tilt $u \in \mathbb{R}^d$. In the case of non-convex W, uniqueness of the ergodic gradient component can be violated, for tilt $u = 0$. We discuss in [4] recent extensions of the results in [2]. In [4] we are using better finite range decomposition techniques to tackle the loss of regularity in [2]. The main topic is the Gaussian decay of the two-point correlation functions for the class of non-convex potentials studied in [2] which has been done in [1] for small tilts and large inverse temperature. We finally discuss the scaling limit to the continuum GFF for the class non-convex potentials studied in [2, 4], in particular we are confident to prove the conjecture that the variance of the continuum GFF is given by the Hessian of the surface tensions for the small tilt and large inverse temperature. The prove of the latter statement requires a careful renormalisation group analysis of the quotient of partition functions using the strict convexity of the corresponding surface tension in [2] and an expansion of involving non-constant tilt conditions.

References

[1] S. Adams, *Gaussian decay of correlations for non-convex potentials*, preprint December (2018).

[2] S. Adams, R. Kotecký and S. Müller, *Strict convexity of the surface tension for non-convex potentials*, 157 pages, arXiv:1606.09541 June (2016).

[3] S. Adams, R. Kotecký and S. Müller, *Finite range decomposition for families of gradient Gaussian measures*, Journal of Functional Analysis **264**, 169–206 (2013).

[4] S. Adams, S. Buchholz, R. Kotecký and S. Müller, *Cauchy-Born Rule from Microscopic Models with Non-convex Potentials*, in preparation (2018).

Three diffraction snippets

Michael Baake

Via three short examples, some persistent problems and recent developments in diffraction theory are presented. In particular, hyperuniformity via scaling near the origin, the inverse problem in the presence of absolutely continuous spectrum, and the coexistence of long-range order and entropy are addressed.

Scaling near the origin. The analysis of patch fluctuations in Delone and more general point sets in Euclidean space are connected with the scaling behaviour of the total diffraction intensity near the origin. In one dimension, detailed studies have been made in the context of aperiodic systems [5]. Several of the results were rediscovered and extended more recently in [6], though some proofs are still missing.

For regular model sets in $\mathbb{R}$ with Euclidean internal space of dimension one and an interval as a window (see [1] for general background), the generic scaling behaviour of the diffraction measure $\widehat{\gamma}$ is given by

$$\widehat{\gamma}\big((0,x]\big) \,=\, \mathcal{O}(x^2) \qquad \text{as } x \to 0.$$

This behaviour ultimately emerges from $\frac{\sin(z)}{z} = \mathcal{O}(z^{-1})$ as $z \to \infty$, where the relation between z and x results from the $\star$-map of the projection formalism. Interestingly, for special values of the length of the interval, one finds the faster decay $\widehat{\gamma}\big((0,x]\big) = \mathcal{O}(x^4)$ as $x \to 0$. This is due to sampling $\frac{\sin(z)}{z}$ along a sequence of points that lie near the zeros of $\sin(z)$ and thus lead to a faster decay rate. All cases where this phenomenon occurs are related to an underlying *inflation symmetry* of the system, which has strong spectral consequences via an exact renormalisation relation; see [2] and references therein.

An isospectral family. The classic, binary Rudin–Shapiro (RS) sequence, which was earlier described by Golay (see [1] and references therein), provides a deterministic example of a weighted point set with linear complexity (hence zero entropy) and vanishing two-point correlations. Choosing weights of opposite sign, ± 1 say, leads to a bi-infinite sequence $w = (w_i)_{i\in\mathbb{Z}}$ with the corresponding diffraction measure $\widehat{\gamma}$ simply being Lebesgue measure. In particular, one then has $\widehat{\gamma}\big((0,x]\big) = x$ for any $x > 0$.

A *Bernoullisation* is achieved by randomly flipping the sign of w_i, independently for each $i \in \mathbb{Z}$, with probability $p \in \big[0, \frac{1}{2}\big]$. Here, $p = 0$ is the deterministic RS sequence, while $p = \frac{1}{2}$ gives a fair coin tossing sequence with entropy $\log(2)$. The entropy changes continuously from 0 to $\log(2)$ as one increases p, while the diffraction measure almost surely (in the sense of the underlying Bernoulli process) remains unchanged, which means that we have an isospectral family. In this family, diffraction is totally blind to entropy, and it is clear that the inverse problem of structure determination becomes more complicated in such a situation.

Random Inflations. The classic Fibonacci substitution [1] defined by $a \mapsto ab$ and $b \mapsto a$ on the binary alphabet $\mathcal{A} = \{a, b\}$ results in an aperiodic, symbolic dynamical system of Sturmian type, hence with minimal complexity $n + 1$ for the number of subwords of length n. The same hull is obtained from the variant

$b \mapsto a \mapsto ba$. Matters change when $a \mapsto ab$ or $a \mapsto ba$ are applied randomly and independently for every letter of type a (together with $b \mapsto a$ always). This defines a new hull with positive entropy, which is known [4] to be

$$s = \sum_{n=2}^{\infty} \frac{\log(n)}{\tau^{n+2}} \approx 0.444\,399, \quad \text{where } \tau = \frac{1+\sqrt{5}}{2}.$$

The precise nature of this number s is unknown.

Now, if one realises each symbolic sequence as a tiling with two interval types of fixed length, each realisation of this kind results in a system with long-range order — despite the fact that one has positive entropy. This applies to *all* elements of the hull, and not just to almost all as one might expect. More precisely, the diffraction spectrum (as well as the dynamical spectrum) is of mixed type, with a pure point and an absolutely continuous component, but no singular continuous one [3]. No non-trivial eigenfunction of the corresponding dynamical system (under the translation action of $\mathbb{R}$) is continuous, though they all are when restricted to a suitable subset of the hull of full measure. This coexistence of long-range order and entropy seems an important property that is relevant for applications in physics, but has not been understood very well so far.

References

[1] M. Baake and U. Grimm, *Aperiodic Order. Vol. 1. A Mathematical Invitation*, Cambridge University Press, Cambridge (2013).

[2] M. Baake, U. Grimm and N. Mañibo, *Spectral analysis of a family of binary inflations rules*, Lett. Math. Phys. **108** (2018) 1783–1805; `arXiv:1709.09083`.

[3] M. Baake, T. Spindeler and N. Strungaru, *Diffraction of compatible random substitutions in one dimension*, Indag. Math. **29** (2018) 1031–1071; `arXiv:1712.00323`.

[4] C. Godrèche and J.M. Luck, *Quasiperiodicity and randomness in tilings of the plane*, J. Stat. Phys. **55** (1989), 1–28.

[5] C. Godrèche and J.M. Luck, *Multifractal analysis in reciprocal space and the nature of the Fourier transform of self-similar structures*, J. Phys. A: Math. Gen. **23** (1990) 3769–3797.

[6] E.C. Oğuz, J.E.S. Socolar, P.J. Steinhardt and S. Torquato, *Hyperuniformity and anti-hyperuniformity in one-dimensional substitution tilings*, Acta Cryst. A, in press; preprint `arXiv:1806.10641`.

Finite-difference discretization of the Ambrosio-Tortorelli functional

Annika Bach

(joint work with Andrea Braides, Caterina Ida Zeppieri)

The variational approach to problems in image segmentation often leads to the minimization of a so-called free-discontinuity functional, i.e., a functional consisting of competing volume and surface terms. Indeed, the reconstruction of objects and object contours in a possibly distorted grey-scale image $g : \mathbb{R}^n \supset \Omega \to [0,1]$ based on the approach of Mumford and Shah leads to minimizing the functional

$$MS(u) + \int_\Omega |u-g|^2\,dx = \int_\Omega |\nabla u|^2\,dx + \mathcal{H}^{n-1}(S_u) + \int_\Omega |u-g|^2\,dx$$

in the space $SBV(\Omega)$. Here S_u denotes the jump set of u. Unfortunately, it is notoriously difficult to minimize MS numercially. In order to bypass these difficulties, Ambrosio and Tortorelli [1, 2] provide an approximation of MS in the sense of Γ-convergence via the sequence of elliptic functionals

$$AT_\varepsilon(u,v) = \int_\Omega v^2 |\nabla u|^2 \, dx + \frac{1}{2} \int_\Omega \frac{(v-1)^2}{\varepsilon} + \varepsilon |\nabla v|^2 \, dx,$$

defined for $u, v \in W^{1,2}(\Omega)$. These functionals are now ready for numerical implementation using, e.g., finite elements or finite differences. According to [4] a finite-elements discretization of AT_ε preserves the convergence to the Mumford-Shah functional provided that the discretization step-size $\delta = \delta(\varepsilon)$ satisfies $\delta \ll \varepsilon$. It is, however not clear if this condition holds always true in the numerical implementation. Indeed, here it might also happen that δ and ε are comparable. Then one would expect that the underlying mesh should affect the Γ-limit as it is the case, e.g., in the discretization of the Modica-Mortola functionals analyzed in [5].

Motivated by the analysis carried out in [5], in [3] we consider a finite-difference discretization of the Ambrosio-Tortorelli functionals defined as

$$E_\varepsilon(u,v) = \frac{1}{2} \left(\sum_{\substack{i,j \in \Omega \cap \delta\mathbb{Z}^n \\ |i-j|=\delta}} \delta^n (v^i)^2 \left| \frac{u^i - u^j}{\delta} \right|^2 + \sum_{i \in \Omega \cap \delta\mathbb{Z}^n} \delta^n \frac{(v^i-1)^2}{\varepsilon} + \frac{1}{2} \sum_{\substack{i,j \in \Omega \cap \delta\mathbb{Z}^n \\ |i-j|=\delta}} \varepsilon \delta^n \left| \frac{v^i - v^j}{\delta} \right|^2 \right)$$

and we analyze its asymptotic behavior as ε and δ simultaneously tend to zero. More precisely, if $\ell = \lim_\varepsilon \frac{\delta}{\varepsilon}$ then [3, Theorem 2.1] determines the Γ-limit E_ℓ of the sequence (E_ε) in all the three scaling regimes $\ell = 0$, $\ell \in (0, +\infty)$, $\ell = +\infty$. In fact, we show that $E_0(u) = MS(u)$ as in [4], while for $\ell \in (0, +\infty)$ and $n = 2$ the Γ-limit is an anisotropic free-discontinuity functional of the form

$$E_\ell(u) = \int_\Omega |\nabla u|^2 \, dx + \int_{S_u} \varphi_\ell(\nu_u) \, d\mathcal{H}^1, \tag{1}$$

for some surface integrand φ_ℓ depending on the approximate normal ν_u to S_u. Finally, in the regime $\ell = +\infty$ the Γ-limit is finite only on $W^{1,2}(\Omega)$ and is given by the Dirichlet part of the energy, i.e., $E_\infty(u) = \int_\Omega |\nabla u|^2 \, dx$.

We notice that while the Γ-limit in the two extreme regimes $\ell = 0$ or $\ell = +\infty$ can be computed explicitly using slicing and blow-up techniques, in the critical case $\ell \in (0, +\infty)$ we first use an abstract argument to prove that up to subsequences the Γ-limit exists and can be represented as an integral functional [3, Theorems 5.3, 5.5]. Based on this result we show that if $n = 2$ the whole sequence (E_ε) Γ-converges to the functional E_ℓ given by (1) and we also provide an explicit formula for the surface integrand φ_ℓ, which reflects the geometry of the underlying lattice.

References

[1] L. Ambrosio and V. M. Tortorelli, *Approximation of functionals depending on jumps by elliptic functionals via* Γ*-convergence*, Comm. Pure Appl. Math. **43** no. 8 (1990), 999–1036.

[2] L. Ambrosio and V. M. Tortorelli, *On the approximation of free-discontinuity problems*, Boll. Un. Mat. Ital. (7) **6-B** (1992), 105–123.

[3] A. Bach, A. Braides, and C. I. Zeppieri, *Quantitative analysis of finite-difference approximations of free-discontinuity problems*, submitted. http://cvgmt.sns.it/paper/3923/.
[4] G. Bellettini and A. Coscia, *Discrete approximation of a free discontinuity problem*, Numer. Funct. Anal. and Optimiz. **15** (1994), 201–224.
[5] A. Braides and A. Yip, *A quantitative description of mesh dependence for the discretization of singularly perturbed nonconvex problems*, SIAM J. Numer. Anal. **50** no. 4 (2012), 1883–1898.

Soft Lattice Theta Functions

Laurent Bétermin
(joint work with Hans Knüpfer, Universität Heidelberg)

We study the Gaussian energy per point of masses, given by radially symmetric probability measures, located on lattices. More precisely, we investigate the minimality properties of the Soft Lattice Theta Functions defined by

$$\theta_{\mu_L+\nu_z}(\alpha) := \sum_{p\in L} \iint_{\mathbb{R}^d\times\mathbb{R}^d} e^{-\pi\alpha|x+p-z-y|^2} d\mu(x)d\nu(y),$$

where $L = \oplus_{i=1}^d \mathbb{Z}u_i \subset \mathbb{R}^d$ is a Bravais lattice, $z \in \mathbb{R}^d$, $\alpha > 0$ and $\mu, \nu \in \mathcal{P}(\mathbb{R}^d)$ are two radially symmetric probability measures. In particular, two kinds of problems are interesting, for fixed μ, ν and $\alpha > 0$:

(P1) What is the minimizer of $L \mapsto \theta_{\mu_L+\nu_z}(\alpha)$ among Bravais lattices of fixed density? That corresponds to find the optimal crystal structure that minimizes the Gaussian energy.
(P2) What is the minimizer of $z \mapsto \theta_{\mu_L+\nu_z}(\alpha)$ on the unit cell Q_L of a given lattice L? That corresponds to find the optimal location of a mass that has the lowest Gaussian interaction energy with the smeared out lattice L.

Those problems have been investigated in the Dirac masses case, i.e. the minimization of the lattice theta function and the translated theta function defined by

$$L \mapsto \theta_L(\alpha) := \sum_{p\in L} e^{-\pi\alpha|p|^2}, \quad \text{and} \quad z \mapsto \theta_{L+z}(\alpha) := \sum_{p\in L} e^{-\pi\alpha|p+z|^2},$$

in [8, 9, 6, 7, 5, 2], and several results are now known, including:

(1) The optimality of the triangular lattice Λ_1 among Bravais lattices of unit density for $L \mapsto \theta_L(\alpha)$ and any fixed $\alpha > 0$.
(2) The local minimality of the FCC (resp. BCC) lattice, among Bravais lattices of unit density, for $L \mapsto \theta_L(\alpha)$, if α is large (resp. small) enough, as well as for some discrete values of α.
(3) The minimality of the BCC lattice among Body-Centred-Orthorhombic lattices of unit density, for some discrete values of α.
(4) The local minimality of D_4, E_8 and the Leech lattice, among Bravais lattices of unit density, for $L \mapsto \theta_L(\alpha)$ in dimensions $\{4, 8, 24\}$.

(5) The minimality of the center of Q_L, when $L \subset \mathbb{R}^d$ is an orthorhombic lattice, for $z \mapsto \theta_{L+z}(\alpha)$ and any fixed $\alpha > 0$.
(6) The minimality of the two barycenters of the primitive triangles composing the unit cell of the triangular lattice Q_{Λ_1}, for $z \mapsto \theta_{L+z}(\alpha)$ and any fixed $\alpha > 0$.

In [4], we have shown that (1), i.e. the optimality of the triangular lattice, stays true for $L \mapsto \theta_{\mu_L+\nu_z}(\alpha)$ if μ, ν are absolutely continuous with respect to the Lebesgue measure and with a density $x \mapsto \rho(|x|^2)$ where ρ is a completely monotone function (let us call CM such measures), or if μ, ν are sufficiently rescaled around the lattice points. The proof is based on an approximation argument which we have adapted in [3] for any dimension and for the translated theta function, proving that the known results (1)–(6) for (P1) and (P2) stay true for CM measures or if they are enough rescaled around the points, exactly as previously explained in the triangular lattice case.

Furthermore, both Sarnak-Strömbergsson [9] and Cohn-Kumar's [6] conjectures also hold for masses interaction:

(CK) For any $\alpha > 0$, the triangular lattice Λ_1 is the unique minimizer of $L \mapsto \theta_{\mu_L+\nu_z}(\alpha)$ among periodic configurations (i.e. union of Bravais lattices) of unit density, if μ, ν are CM measures or enough rescaled around the lattice points.
(SS) If $\alpha > 1$ (resp. $\alpha < 1$), then the FCC (resp. BCC) lattice is the unique minimizer of $L \mapsto \theta_{\mu_L+\nu_z}(\alpha)$ among periodic configurations of unit density, if μ, ν are CM measures or enough rescaled around the lattice points.

References

[1] A. Baernstein II, *A minimum problem for heat kernels on flat tori*, Contemporary Mathematics **201** (1997), 227–243.
[2] L. Bétermin, *Local optimality of cubic lattices for interaction energies*, Analysis and Mathematical Physics (online first), DOI:10.1007/s13324-017-0205-5 (2017), 1–24.
[3] L. Bétermin, *Minimal Soft Lattice Theta Functions*, preprint (2018), arXiv:1809.00473.
[4] L. Bétermin and H. Knüpfer, *Optimal lattice configurations for interacting spatially extended particles*, Letters in Mathematical Physics **108**(10) (2018), 2213–2228.
[5] L. Bétermin and M. Petrache, *Dimension reduction techniques for the minimization of theta functions on lattices*, Journal of Mathematical Physics **58** (2017), 071902.
[6] H. Cohn and A. Kumar, *Universally optimal distribution of points on spheres*, Journal of the American Mathematical Society **20**(1) (2007), 99–148.
[7] R. Coulangeon and A. Schürmann, *Energy Minimization, Periodic Sets and Spherical Designs*, International Mathematical Research Notices **2012** (2012), 829–848.
[8] H.L. Montgomery, *Minimal Theta Functions*, Glasgow Mathematical Journal **30**(1) (1988), 75–85.
[9] P. Sarnak and A. Strömbergsson, *Minima of Epstein's Zeta Function and Heights of Flat Tori*, Inventiones Mathematicae **165** (2006), 115–151.

Understanding the long-range elastic field induced by a crystal defect

Julian Braun
(joint work with Maciej Buze, Hong M. Duong, Thomas Hudson, Christoph Ortner)

Crystalline solids consist of regions of periodic atom arrangements, which are broken by various types of defects. These defects induce long-range displacements fields on the surrounding lattice. E.g., for a straight dislocation, this nonlinear, discrete displacement field is classically approximated by continuum linear elasticity theory (CLE). Much more recently, in [1], the authors have shown how to make such an approximation rigorous starting from atomistic models by providing quantitative error bounds in terms of the distance to the defect core.

In our work, [2, 4], we show how to substantially improve on the CLE far-field description. Indeed, we construct a far field development if higher order approximations. There are two very different types of contribution to such a development. On the one side are terms that can be described by linear elliptic continuum PDEs. These start with the CLE approximation and continue with nonlinear terms, strain gradient terms, etc. On the other side is a vectorial multipole expansion, that describes the far field effects of the atomistic core structure.

This results are shown for point defects and screw dislocations but some numerical evidence is presented, that they still hold true for more general defects if adapted appropriately, even if this can not be shown mathematically.

As special case, we get a rigorous characterisation of the leading order far field displacement field of a point defect, which can not be described in a continuum framework but comes from an effective force dipole of the atomistic core structure around the point defect.

Furthermore, two strong application of this theory are presented. First, the knowledge about the far field can used to understand the convergence of supercell approximations for the energy, a vibrational entropy, and combined give a result on the thermodynamic limit of transition rates in point defect diffusion, see [3]. (The rates considered here are the predictions of harmonic transition state theory.) These results include precise convergence rates. And second, the new descriptions of higher order far field approximations directly lead to a new sequential multiscale algorithm for the computation of crystalline defects. The idea is to start by computing a number of continuum terms in the far-field and then use them as a boundary condition for a fully atomistic computation on a fairly small domain. The multipole expansion can be obtained in a small iteration of this procedure with improved boundary conditions based on the defect force multipoles.

References

[1] V. Ehrlacher, C. Ortner, A. Shapeev *Analysis of Boundary Conditions for Crystal Defect Atomistic Simulations*, 2016.

[2] J. Braun, M. Buze, C. Ortner, *The Effect of Crystal Symmetries on the Locality of Screw Dislocation Cores*, 2017, arXiv:1710.07708.

[3] J. Braun, H. M. Duong, C. Ortner, *Thermodynamic Limit of the Transition Rate of a Crystalline Defect*, 2018, arXiv:1810.11643.
[4] J. Braun, T. Hudson, C. Ortner, *in preparation.*

The Γ-limit of the cut functional on dense graph sequences

Paolo Cermelli
(joint work with Andrea Braides, Simone Dovetta)

Large graphs are nowadays common objects of study, and often their analysis is carried out by studying the asymptotic behavior of sequences of graphs, that either result from generative models or retain some outstanding topological feature of the large graph they are meant to approximate. Further insight can be obtained when appropriate notions of convergence and limit objects of graph sequences are used. In this work we use convergence in cut-norm of graphons to study the asymptotics of the simplest interaction problem in large graphs: the bipartition problem.

The fundamental theory of converging graph sequences and graphons has been developed by Benjamini and Schramm, Lovász, Borgs et al. in [1], [2], [3], [4]: we sketch below some of the basic ideas. Loosely speaking, a graphon is a measurable function $W : [0,1]^2 \to \mathbb{R}$ that is a functional representation of the adjacency matrix of a graph whose nodes fill the interval $[0,1]$. More precisely, consider a sequence of simple graphs $\{G_n\}_{n\in\mathbb{N}}$, let $V(G_n)$ be the vertex set, and A^n_{ij} the adjacency matrix of G_n, and assume that the sequence is a dense graph sequence, i.e., the number of nodes and edges of G_n grow as n and n^2, respectively. We can associate to each G_n a piecewise constant function on $[0,1]^2$ as follows: fix any labeling of the nodes, divide the interval $[0,1]$ in n equal-sized intervals $\{I^n_i\}_{i=1,\dots,n}$, and define the piecewise-constant function W_{G_n} on $[0,1]^2$ by

$$W_{G_n}(x,y) = A_{ij} \quad \text{if} \quad (x,y) \in I^n_i \times I^n_j;$$

if we define the cut norm of a graphon as

$$||W||_\square = \sup_{S,T\subseteq[0,1]} \Big| \int_{S\times T} W(x,y)dxdy \Big|,$$

with the supremum taken over all measurable subsets S, T of $[0,1]$, then we say that the sequence $\{G_n\}_{n\in\mathbb{N}}$ converges to W in the cut norm if

$$||W - W_{G_n}||_\square \to 0 \quad \text{as } n \to +\infty.$$

A fundamental theorem of [6] guarantees that, modulo relabeling, a dense graph sequence always admits a limit graphon.

In this work we study the asymptotic behavior of graph functionals of the simplest form. Namely, for every $n \in \mathbb{N}$ consider the cut-functional

$$\tilde{F}_n(\tilde{u}) = \frac{1}{n^2} \sum_{i,j\in V(G_n)} A^n_{ij} |\tilde{u}(i) - \tilde{u}(j)|^2, \tag{1}$$

where $\tilde{u} : V(G_n) \to \{-1, +1\}$ is a spin function on G_n. The above functional is the simplest energy functional of a system in which each node can be in a

binary state in $\{-1,1\}$ and the interactions between nodes are described by the adjacency matrix of the graph. Specifically, we study the limit as $n \to +\infty$ of the minimization problem

$$\min_{\tilde{u}\in\tilde{E}^n} \tilde{F}_n(\tilde{u}) \quad \text{with} \quad \tilde{E}^n := \Big\{\tilde{u} : V(G_n) \to \{-1,+1\} : \sum_{i\in V(G_n)} \tilde{u}(i) = 0\Big\}. \tag{2}$$

This minimum problem has a natural interpretation in terms of the bisection problem for the graphs G_n, an important problem in applications. Indeed, letting

$$S_n = \{i \in V(G_n) : \tilde{u}(i) = +1\}, \qquad S_n^c = V(G_n) \setminus S_n,$$

then the only non-vanishing terms in (1) are those that involve pairs of nodes i, j such that either $i \in S_n$ and $j \in S_n^c$ or $j \in S_n$ and $i \in S_n^c$, so that, granted the symmetry of the adjacency matrix, we can write

$$\tilde{F}_n(\tilde{u}) = \frac{8}{n^2} \sum_{i\in S_n, j\in S_n^c} A_{ij}^n = \frac{8}{n^2} e_{G_n}(S_n, S_n^c),$$

where $e_{G_n}(S_n, S_n^c)$ is the number of edges that connect S_n to S_n^c. Hence, the minimization of the functional (1) over spin functions in $\tilde{E}^n$ is equivalent to finding the subdivision of $V(G_n)$ into equal parts that minimizes the size of the cut between the two communities S_n and S_n^c.

To study the asymptotic behaviour of the minimization problems (2) we compute the Γ-limit of the sequence of cut functionals (1). Indeed, Γ-convergence guarantees that the minima of the cut functionals converge to the minima of their limit [5].

Our main result is the representation, in terms of Young measures, of the Γ-limit of a sequence of cut functionals of quite general form, that allows to study the multi-partition problem in the dense-graph limit. The Γ-limit of functionals (1) admits the representation

$$I(\nu) = \int_{[0,1]^2} W(x,y)\Big(\int_{\mathbb{R}^2} |\lambda-\mu|^2 d\nu_x(\lambda) d\nu_y(\mu)\Big) dxdy, \tag{3}$$

where the kernel $W(x,y)$ is the limit graphon associated to the sequence of graphs $\{G_n\}_{n\in\mathbb{N}}$, and ν_x is a spin Young measure on $[0,1]$, i.e., a probability measure with support on $\{-1,1\}$, parametrized by $x \in [0,1]$. The interval $[0,1]$ plays here the role of the set of nodes of the graph in the limit.

The fact that the bisection problem has a solution in terms of a probability measure reflects the fact that, when the graph has a large number of connections, the distinction between the communities can be blurry, and what makes sense is just to compute the probability that a node belongs to one of the two communities.

The limit functional (3) admits a simpler representation, noting that Young measures with support in $\{-1,1\}$ can be written as

$$\nu_x = \theta(x)\delta_1 + (1-\theta(x))\delta_{-1} \text{ for almost all } x \in [0,1],$$

with $\theta : [0,1] \to [0,1]$ a measurable function. In terms of θ, the limit cut functional becomes

(4)

$$J(\theta) = \begin{cases} 8 \displaystyle\int_{[0,1]^2} W(x,y)\theta(x)(1-\theta(y))dxdy & \theta \in L^\infty([0,1],[0,1]) \\ +\infty & \theta \in L^\infty([0,1]) \setminus L^\infty([0,1],[0,1]). \end{cases}$$

The above form of the cut functional allows to explicitly compute the minimal-cut bisections once the appropriate graphon is given: an example is given in the Figure below.

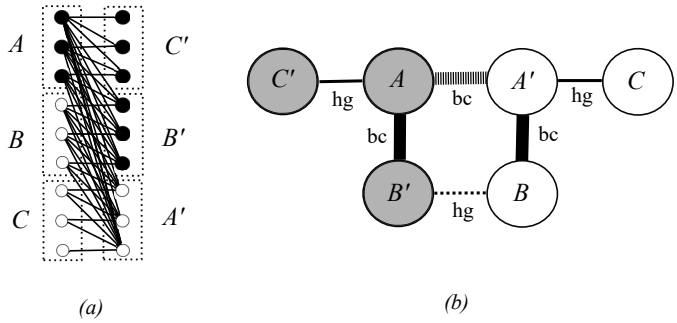

FIGURE 1. The structure of the optimal bipartition in the half graph. (a): standard representation; (b): a schematic representation of the communities: 'hg' stands for a half-graph connectivity between two communities of size k (involving $k(k+1)/2$ edges), while 'bc' stands for a complete bipartite connectivity (k^2 edges). Dashed lines are the cuts.

REFERENCES

[1] I. Benjamini, O. Schramm; Recurrence of distributional limits of finite planar graphs, *Electronic Journal of Probability*, **6**/23, 1-13 (2001).

[2] L. Lovász, B. Szegedy; Limits of dense graph sequences, *Journal of Combinatorial Theory, Series B*, **96**, 933-957 (2006).

[3] C. Borgs, J.T. Chayes, L. Lovász, V.T. Sós, K. Vesztergombi; Convergent Sequences of Dense Graphs I. Subgraph frequencies, metric properties and testing, *Advances in Mathematics*, **219**/6, 1801-1851 (2008).

[4] L. Lovász; Large networks and graph limits, *American Mathematical Society Colloquium Publications* **60**, (2012).

[5] A. Braides; A handbook of Γ-convergence, *Handbook of Differential, Equations – Stationary Partial Differential Equations* **3**, 101-213 (2006).

[6] L. Lovász, B. Szegedy; Szemerédi's lemma for the analyst, *Geometric and Functional Analysis*, **17**/1252-270 (2007).

A maximal fluctuation estimate of Wulff shapes on 2d lattices

Marco Cicalese
(joint work with Gian Paolo Leonardi)

Let $\mathcal{L}$ be a periodic lattice in $\mathbb{R}^2$ of spacing 1 and degree l; i.e.,

$$\min\{|x-y|,\, x,y\in\mathcal{L}\}=1,$$
$$\#\{y\in\mathcal{L}:\,|x-y|=1\}=l,\forall x\in\mathcal{L}.$$

For a given configuration of N lattice points, say $X=\{x_1,x_2,\dots,x_N\}\in\mathcal{L}^N$, we define the function $b: X\mapsto\mathbb{N}$ which assigns to each $x\in X$ the number of its loose bonds, that is the number of its nearest neighbours that do not belong to X, namely

$$b(x)=l-\#\{y\in X:\,|x-y|=1\}.$$

We define the energy of the configuration X as

$$E_N(X)=\sum_{i=1}^N b(x_i).$$

At leading order such an energy agrees with the so called Gibbs excess energy of N atoms which crystallise on the lattice $\mathcal{L}$ and occupy the positions of the configuration X. According to the Gibbs theory, as N grows low energy microscopic configurations converge in an appropriate sense to the shape of a macroscopic crystal grain.

For $x\in\mathcal{L}$ we define $V(x)=\{y\in\mathbb{R}^2:\,|y-x|\le|y-z|,\,z\in\mathcal{L}\}$ to be the Voronoi cell of the lattice point x. To any configuration $X\in\mathcal{L}^N$ we associate the Voronoi set $V(X)=\bigcup_{i=1}^N V(x_i)$. It is well known (see for instance [1]) that, as $N\to\infty$ the ground states of E_N, say Y are not unique and converge (in the L^1 sense of the characteristic functions of $\frac{1}{N}V(\frac{Y}{\sqrt{N}})$) to the unique Wulff shape associated to an anisotropic perimeter functional of the type

$$\mathcal{P}_{\mathcal{L}}(E)=\int_{\partial^* E}\varphi_{\mathcal{L}}(\nu_E)\,d\mathcal{H}^1,$$

and satisfying the constraint $|W|=|V(X)|$. In the formula above $\varphi_{\mathcal{L}}: S^1\to[0,+\infty)$ is a 1-homogeneous function such that $\{x\in\mathbb{R}^2:\,\varphi_{\mathcal{L}}(x)\le 1\}$ is a polygon whose anisotropy reflects the anisotropy of the lattice. The estimate of the rate of convergence of the Voronoi set of a (almost) minimum of E_N to the Wulff shape W_N of the limit functional with the same Lebesgue measure ($|W_N|=|V(X)|$), takes the name of maximal fluctuation estimate. The following holds true:

Theorem 1. *Let $X\in\mathcal{L}^N$ and $\alpha_N>0$ be such that*

$$E_N(X)-\min E_N(X)\le\alpha_N.$$

Then, there exists a universal constant $C>0$ such that

$$\min\{|V(X)\triangle(x+W_N)|,\,x\in\mathbb{R}^2\}\le C\,N^{3/4}\sqrt{1+\alpha_N}.$$

As a corollary, if X is a minimum of E_N, in which case $\alpha_N = 0$, we obtain the so-called $N^{3/4}$-law (see [2, 3, 5, 7]). The theorem above is proved reducing the maximal fluctuation estimate to a sharp quantitative isoperimetric inequality for crystalline perimeters proved in [4]. As a final comment, we notice that a similar soft argument can be used also in higher dimension, but it does not lead to the sharp fluctuation estimate for minimisers. For instance in the case $\mathcal{L} = \mathbb{Z}^3$ it would give the scaling $N^{5/6}$, while it has been recently proved in [6] that in this case the optimal scaling remains $N^{3/4}$.

References

[1] R. Alicandro, A. Braides, M. Cicalese, *Phase and anti-phase boundaries in binary discrete systems: a variational viewpoint*, Networks and Heterogeneous Media, **1**, (2006), 85–107.

[2] E. Davoli, P. Piovano and U. Stefanelli, *Sharp $N^{3/4}$ Law for the Minimizers of the Edge-Isoperimetric Problem on the Triangular Lattice*, Journal of nonlinear science, **27**, (2017), 627–660.

[3] E. Davoli, P. Piovano and U. Stefanelli, *Wulff shape emergence in graphene*, Mathematical Models and Methods in Applied Sciences, **26**, (2016), 2277–2310.

[4] A. Figalli, F. Maggi and A. Pratelli, *A mass transportation approach to quantitative isoperimetric inequalities*, Inventiones mathematicae, **182**, (2010), 167–211.

[5] E. Mainini, P. Piovano and U. Stefanelli, *Finite crystallization in the square lattice*, Nonlinearity, **27**, (2014), 717–737.

[6] E. Mainini, P. Piovano, B. Schmidt and U. Stefanelli,, *$N^{3/4}$ law in the cubic lattice*, arXiv preprint arXiv:1807.00811, (2018).

[7] B. Schmidt, *Ground states of the 2D sticky disc model: fine properties and $N^{3/4}$ law for the deviation from the asymptotic Wulff shape*, Journal of Statistical Physics, **153**, (2013), 727–738.

Γ-convergence of the Heitmann-Radin sticky disc energy to the crystalline perimeter

Lucia De Luca

(joint work with Matteo Novaga, Marcello Ponsiglione)

The sticky disc model has been introduced by Heitmann and Radin [2] and is the most basic potential mimicking attraction at long range and repulsion at short range. In such a model, particles are identified with impenetrable spheres (sticky discs) which maximize the number of their contact points. Given N discs in the plane, all of them having diameter equal to one and centered at points $x_1, \dots, x_N$, the corresponding Heitmann-Radin energy is given by

$$E(x_1, \dots, x_N) := \frac{1}{2} \sum_{i \neq j} V(|x_j - x_i|)\,,$$

where V is the sticky disc potential defined by

$$V(r) := \begin{cases} +\infty & \text{if } r < 1\,, \\ -1 & \text{if } r = 1\,, \\ 0 & \text{if } r > 1\,. \end{cases}$$

Together with the soft-disc affine case treated in [7], this is the only two dimensional model for which finite positional crystallization has been proven, i.e., it has been shown that for every $N \in \mathbb{N}$, the minimizers of the energy E among the configurations $X_N = \{x_1, \dots, x_N\}$ are subsets of a unique equilateral triangular lattice with unitary lattice spacing. The first proof of this result has been provided in [2] and it exploits an ansatz on the exact value of the minimal energy, which is

$$E_N = -[3N - \sqrt{12N - 3}]\,,$$

where $[x]$ denotes the greatest integer less than or equal to the real number x. Roughly speaking, the minimal energy consists of a bulk term that is equal to $-3N$ and of a perimeter term which is proportional to $\sqrt{N}$.

Here we consider the asymptotic behavior of the energy E in the perimeter-scaling regime, without assuming that the particles lie on a reference lattice, i.e., we consider particle configurations $X_N = \{x_1, \dots, x_N\} \subset \mathbb{R}^2$ such that

$$E(X_N) + 3N \leq C\sqrt{N}. \tag{1}$$

To any particle configuration X_N we associate an empirical measure $\mu_N = \sum_{i=1}^{N} \delta_{\frac{x_i}{\sqrt{N}}}$ and a piecewise constant orientation θ_N defined on the triangular faces of the discrete graph generated by the configuration X_N (in the spirit of [3]). We prove that in the regime (1), the measures μ_N converge - as $N \to \infty$ - to $\mathbb{1}_\Omega \mathrm{d}x$ for some set Ω of finite perimeter. Such a result had already been proven in [1], using a more general interaction potential and assuming that the graph is connected. However, the main novelty of our result concerns with the compactness for the orientation variable θ_N. Indeed, we show that the orientations θ_N converge to some $\theta \in SBV(\Omega)$, where $\theta = \sum_{j \in J} \theta_j \mathbb{1}_{\omega_j}$ with $J \subseteq \mathbb{N}$ and $\{\omega_j\}_j$ being a Caccioppoli partition of Ω. Here each ω_j represents a grain of the polycrystal Ω, endowed with orientation θ_j.

Roughly speaking, we prove that the Heitmann-Radin energy enforces crystallization not only for minimizers, but also for configurations satisfying (1). But while for minimizers the orientation of the underlying lattice is constant, for almost minimizers global orientation can be disrupted, giving rise to polycrystalline structure.

Moreover, we compute the Γ-limit of the energy functionals whenever the limit orientation (but not the orientation for finite N) is constant, i.e., in the case of a single crystal $\theta = \bar{\theta}\mathbb{1}_\Omega$. In this case the Γ-limit is given by the anisotropic perimeter of Ω, where the anisotropy corresponds to a Finsler metric whose Wulff shapes are hexagons with orientation $\bar{\theta}$. The proof of the Γ-liminf inequality exploits the representation formulas, introduced in [3], that allow to rewrite the Heitmann-Radin energy in terms of the discrete perimeter of the graph generated by the particles.

For polycrystals, where the orientation is not constant, one expects some additional surface contribution, induced by grain boundaries. The sharp grain boundary energy, and in turn the Γ-limit in the general case, are not available at the present. Nevertheless, we provide upper and lower bounds for the energy also in

the case of polycrystals. On the one hand, such bounds, although non optimal, are enough to show that, depending on the (macroscopic) shape of the limit set Ω, both the single crystal and the polycrystalline structure could be energetically favorable. On the other hand, according to the lower bound, the energy at grain boundaries is larger than a positive constant which does not depend on the magnitude of the jump $[\theta]$ of the orientation function. This is in contrast with the Read-Shockley formula [8], which predicts that the energy density at grain boundaries is proportional to $|[\theta]|\log(|[\theta]|)$. In this respect, the sticky disc model predicts a grain boundary energy higher than the one for real crystals, where elastic deformations together with edge dislocations decrease the number of atoms with wrong coordination number, relaxing the energy density to lower states [6, 5].

Therefore, a natural question is whether our results can be extended to more general interaction potentials, which are less rigid and take into account also elastic deformations. A first step in this direction would be to consider the soft-disc affine potential in [7].

For Lennard Jones type potentials, in [9] it is proven that the asymptotic energy density of minimizers is consistent with that of the regular triangular lattice. To our knowledge, our result is the first providing asymptotic (local) crystallization by compactness arguments for almost minimizers of some explicit canonical, although very simple and rigid, interaction potential.

The results presented here are proven in [4].

References

[1] Y. Au Yeung, G. Friesecke, B. Schmidt, *Minimizing atomic configurations of short range pair potentials in two dimensions: crystallization in the Wulff shape*, Calc. Var. Partial Differ. Equ. **44** (2012), 81–100.

[2] R. C. Heitmann, C. Radin, *The ground state for sticky disks*, J. Stat. Phys. **22** (1980), 281–287.

[3] L. De Luca, G. Friesecke, *Crystallization in two dimensions and a discrete Gauss-Bonnet theorem*, J. Nonlinear Sci. **28** (2018), 69–90.

[4] L. De Luca, M. Novaga, M. Ponsiglione, Γ-*convergence of the Heitmann-Radin sticky disc energy to the crystalline perimeter*, to appear in J. Nonlinear Sci. .

[5] S. Fanzon, M. Palombaro, M. Ponsiglione, *Derivation of linearised polycrystals from a 2D system of edge dislocations*, Preprint 2018. ArXiv: 1805.04484.

[6] G. Lauteri, S. Luckhaus, *An energy estimate for dislocation configurations and the emergence of Cosserat-type structures in metal plasticity*, Preprint 2017, ArXiv: 1608.06155.

[7] C. Radin, *The ground states for soft discs*, J. Stat. Phys. **26** (1981), 365–373.

[8] W. T. Read, W. Shockley, *Dislocation models of crystal grain boundaries*, Phys. Rev. **78** (1950) 275–289.

[9] F. Theil, *A proof of crystallization in two dimensions*, Comm. Math. Phys. **262** (2006), 209–236.

Ripples in graphene: A variational approach

Manuel Friedrich
(joint work with Ulisse Stefanelli)

Graphene is a one-atom thick layer of carbon atoms arranged in a regular hexagonal lattice whose serendipitous discovery in 2005 sparkled research on two-dimensional materials systems. Graphene is locally two-dimensional but not flat: wavy patterns on the scale of approximately one hundred atom spacings have been experimentally identified [4] and computationally investigated [1]. Whereas nanoscale ripples appear in suspended samples, free graphene samples in absence of support have the tendency to roll-up in tube-like structures. Besides the academic interest, the understanding of the fine geometry of graphene sheets is of a great applicative significance since it is regarded to be the relevant scattering mechanism limiting electronic mobility.

The goal of the papers [2, 3] is to address the phenomenon of rippling and rolling-up in graphene by identifying global minimizers of configurational energies in the frame of Molecular Mechanics. The actual configuration of a graphene sheet is identified with a three-dimensional deformation of the ideal hexagonal lattice. To each deformation, we associate an energy which is the sum over *cell energies* of the form

$$E_{\rm cell}(y_1,\dots,y_6)=\frac{1}{2}\sum_{i=1}^{6} v_2(|y_i-y_{i-1}|)+\sum_{i=1}^{6} v_2(|y_i-y_{i-2}|)+\sum_{i=1}^{6} v_3(\theta_i),$$

where $\{y_1,\dots,y_6\}$ denote the actual positions of six atoms $\{x_1,\dots,x_6\}$ in the reference configuration corresponding to a simple cycle in the hexagonal graph (arranged counterclockwise). Here, the first two terms correspond to *nearest-neighbors* and *next-to-nearest-neighbors*, respectively, and by θ_i we indicate the *bond angle* at y_i formed by the segments $\{y_{i+1},y_i\}$ and $\{y_{i-1},y_i\}$ which is less or equal to π. The *two-body* interaction potential v_2 is supposed to be short-range repulsive and long-range attractive with its minimum value attained only at 1. On the other hand, the *three-body* interaction density v_3 is assumed to attain the minimum value only at $2\pi/3$, reflecting $sp2$ covalent bonding in carbon, see [5].

An elementary argument shows that a deformation is a ground state if and only if the cell energy of each hexagonal cell is minimized. It turns out that, for minimizers of the cell energy, all bonds have length $\ell^*\le 1$ and all angles have amplitude $\theta^*<2\pi/3$. In particular, this gives rise to two different optimal cell geometries which are both nonplanar. Identifying ground-state deformations then consists in understanding how these optimal cell geometries can be combined to globally admissible deformations.

The main result of the paper [2] provides a complete classification of ground-state deformations of the hexagonal lattice. By exploiting the geometric compatibility of the cell geometries, we prove that all energy minimizers are either periodic in one direction, as in the case of ripples, or rolled up, as in the case of nanotubes. In particular, the result shows that the geometry of minimizers

is completely determined by sections which are orthogonal to the direction along which the configurations are periodic.

In [3], we refine the analysis further and investigate the emergence of specific wave patterning for such orthogonal sections (and hence for the whole three-dimensional configurations). The occurrence of rolled-up ground states can be avoided by additionally imposing periodic boundary conditions, which experimentally corresponds to clamp the edges of a suspended graphene sample. Still, a large variety of energy minimizers with many different (nonperiodic) geometries is possible.

Therefore, we specialize the description via a *generalized energy* which additionally takes longer-range interactions (third neighbors) into account. This choice of the energy leads to a finer characterization of energy minimizers since the energy accounts also for curvature changes of the section. More precisely, the main result of [3] states that, up to lower-order terms, almost minimizers of the energy can be viewed as compositions of waves with a specific optimal wavelength. Here, the crucial point is that this wavelength is independent of the size of the system, which corresponds to experimental and computational findings [1, 4].

References

[1] A. Fasolino, J. H. Los, M. I. Katsnelson. Intrinsic ripples in graphene. Nature Materials, 6 (2007), 858–861.

[2] M. Friedrich, U. Stefanelli. Graphene ground states. Z. Angew. Math. Phys. (2018), 69:70.

[3] M. Friedrich, U. Stefanelli. Periodic ripples in graphene: a variational approach. Submitted, 2018. Preprint at `arXiv:1802.05053`.

[4] J. C. Meyer, A. K. Geim, M. I. Katsnelson, K. S. Novoselov, T. J. Booth, S. Roth. The structure of suspended graphene sheets,. Nature 446 (2007), 60–63.

[5] J. Tersoff. New empirical approach for the structure and energy of covalent systems. Phys. Rev. B, 37 (1988), 6991–7000.

Dynamics of particle systems with a separation constraint

Maria Stella Gelli

(joint work with M. Bongini, M. Novaga)

Starting from the pioneering works [4, 5] the study of the behaviour of large particles systems has gained a lot of popularity thanks also to its connection with many models in applied sciences. Looking at particles as individuals in phenomena of crowd motion or as molecular grains in the framework of fluid mechanics, in this work we are interested in establishing the (asymptotic) dynamics of a system of N-particles interacting through a velocity field V and subject to the physical constraint that their mutual distances cannot be lower than a given threshold $2r$. In this respect each particle can be represented as a rigid bulk disc of radius r (in the reference distance). Depending on the phenomena we would like to reproduce, the velocity field is in general affected by many ingredients such as a singular propulsion potential, a "goal gradient" (due for instance to an exit strategy), a free energy term, etcetera. Here we neglect these additional contributions (that

would be implemented in the model lately) and concentrate on a velocity field of convolution type. This choice relies on the fact that in a crowded flow the velocity of each particle tends to average with those of the neighbouring ones. Despite the fact that a realistic model should take into account stochastic effects in the evolution of the particles, we will only consider the deterministic case. Let us quote that such a model has been largely studied in literature both from a macroscopic and a microscopic point of you, we quote here the work by Venel and Maury [3] and we refer to [7, 2] for an (incomplete) list of references.

More in details, let $N \in \mathbb{N}$ be fixed and, for $i = 1, \dots, N$, let $x_i(t) \in \mathbb{R}^d$ denote the position of the i-particle at time t. In order to have a microscopic flow satisfying the rigid constraint, for a given time interval $[0, T]$, we assume that the flow of $\{x_i^N\},\ i = \dots N$ is ruled by the following system of ODE's:

$$(1) \qquad \begin{cases} \dot{x}_i(t) = \dfrac{1}{N} \displaystyle\sum_{j=1}^{N} H\big(t, x_i(t) - x_j(t)\big) + u_i(t) \\ x_i(0) = x_{0,i}^N \qquad\qquad\qquad\qquad\qquad\qquad\qquad\qquad i = 1, \dots, N, \\ \\ |x_i(t) - x_j(t)| \geq r_N \quad \forall j \neq i \end{cases}$$

where H and $u_1, \dots, u_N$ are Carathéodory functions defined on $[0, T] \times \mathbb{R}^d$ with values in $\mathbb{R}^d$, and r_N is a fixed positive quantity to be chosen later. Here (the convolution with) H is the natural spontaneous velocity of the i-particle suitably modified by the field u_i that accounts for the non-congestion constraint. Moreover the initial positions $\{x_{0,i}^N\},\ i = 1, \dots, N$ satisfy the condition $|x_{0,i} - x_{0,j}| \geq r_N \quad \forall j \neq i$. Let us discuss shortly the meaning of last equation in (1): the positive number r_N depends on N and stands for the minimal distance at which particles are allowed to stay. In the model proposed by Maury and Venel in [3] $r_N = r$ for every N, but that seems unlikely to give rise to something meaningful at the macroscopic scale, where particles can stay arbitrarily close and only density constraints are prescribed. We can thus already see that it ought to be

$$r_N \to 0 \quad \text{as} \quad N \to +\infty.$$

As we are interested in establishing the existence of non-congested flow a natural choice is $r_N \sim 1/N^{\frac{1}{d}}$.

We treat locally Lipschitz vector fields, almost uniformly in time. For such velocities we select u_i of the form $u(t, x_i(t))$, for $u : [0, T] \times \mathbb{R}^d \to \mathbb{R}^d$ as regular as H (see [8]). Existence (and uniqueness) of solutions of the first two equations in (1) for a given time interval $[0, T]$ when $u, H \in W^{1,\infty}$ is in a sense classical. It remains to prove that we can choose the control u in order to satisfy the constraint

$$(2) \qquad |x_i(t) - x_j(t)| \geq r_N \quad \forall j \neq i \qquad i = 1, \dots, N$$

for any time t in the existence interval $[0, T]$.

To this aim we introduce at each step N a functional J_N that is finite only on control u such that (2) is satisfied and that penalizes the L^p-norm of u for some

$p > 1$ and we simply request that the control u_N is such that $J_N(u_N) < +\infty$ (see [6]).

Once existence and compactness of solutions of (1) are established we will study the asymptotic dynamics of $\{x_i^N\}$ as $N \to +\infty$ by looking at the so called empirical measures

$$\rho^N(t) = \frac{1}{N}\sum_{i=1}^{N} \delta_{x_i^N(t)}, \quad \text{for all } t \in [0,T],$$

and taking advantage of the compactness and structure theorems in Ambrosio-Gigli-Savare' for measure-valued absolutely continuous curves (see [1]). Hence, up to subsequences, we take the limit as $N \to +\infty$ in the Wasserstein space of probabilities of the solutions of the discrete convolution-type ODE systems (1). This procedure, also known as *mean-field limit*, allows us to prove for both models the validity of a continuity equation satisfied by the mean field limit. More in detail, the limit measure valued-curves $\rho(t,x)$ are connected with solution of the following Vlasov type equation

$$\begin{cases} \dfrac{\partial \rho}{\partial t}(t,x) = -\mathrm{div}((H * \rho)\rho) \\ \rho(0,x) = \rho_0(x), \end{cases} \tag{3}$$

with the additional feature that the probability measures $\rho(t,\cdot)$ remain absolutely continuous w.r.t. the Lebesgue measure for any time t, and their densities satisfy

$$\rho(t,\cdot) \in L^\infty(\Omega) \text{ for any } t \in [0,T]. \tag{4}$$

Clearly, for a general potential H (or kernel K), we cannot expect solutions of (3) to avoid congestion effects, thus, in order to ensure the validity of the bound (4), our discrete model introduces at the microscopic level the drift terms u_N.

Once we prove the existence of mean field limits, the limit equation (3) should be modified accordingly, in order to take into account the presence of a control term u, limit of the drift terms u_N: more in details the limit equation will be the following

$$\begin{cases} \dfrac{\partial \rho}{\partial t}(t,x) = -\mathrm{div}((H * \rho + u)\rho) \\ \rho(0,x) = \rho_0(x) \end{cases} \tag{5}$$

References

[1] L. Ambrosio, N. Gigli, G. Savare' *Gradient flows in metric spaces and in the space of probability measures*, Lectures in Mathematics ETH Zürich, Birkhaüser (2008).

[2] F. Bolley, J.A. Canizo, J.A. Carrillo, *Sthochastic mean field limit: non Lipschitz forces and swarming*, Math. Models Methods Appl. Sci., **21(11)** (2011), 2179–2210.

[3] B. Maury, J. Venel, *A discrete contact model for crowd motion*, ESAIM: Math. Mod. Num. An., **45(1)** (2011), 145–168.

[4] D. Helbing, *A fluid dynamic model for the movement of pedestrian*, Compl. Syst., **6** (1992), 391–415.

[5] R.L. Hughes, *A continuum theory for the flow of pedestrian*, Transp. Res. B, **36** (2002), 507–535.

[6] M. Bongini, G. Buttazzo, *Optimal control problems in transport dynamics*, Math. Models Methods Appl. Sci., **27(03)** (2017), 427–451.
[7] B. Maury, A. Roudneff-Chupin, F. Santambrogio, *A microscopic crowd motion model of gradient flow type*, Math. Models Methods Appl. Sci., **20(10)** (2010), 1787–1821.
[8] M. Fornasier, F. Solombrino, *Mean-field optimal control*, ESAIM Control Optim. Calc. Var., **20(4)** (2014), 1123–1152.

Hyperuniformity on the Sphere

Peter J. Grabner
(joint work with Johann S. Brauchart and Wöden B. Kusner)

Hyperuniformity has been introduced in [9] as a concept to measure the transition between order and disorder in physical materials. The general idea is to assess intermediate states between perfect crystalline order, quasi-crystalline order, intermediate configurations like jammed packings, and the disorder in amorphous materials by measuring the local density fluctuations expressed by the number variance introduced below. The original work on the subject deals with idealised infinite particle systems.

Our work starts the investigation of a similar concept for sequences of finite point sets on compact spaces, especially the sphere $\mathbb{S}^d \subset \mathbb{R}^{d+1}$. The notion of hyperuniformity can either be used to analyse the finer distribution behaviour of deterministically constructed point sets (see [4]) as well as to describe the local behaviour of point processes (see [5]). It turns out that determinantal point processes typically exhibit hyperuniform samples, whereas the notion is built so that i.i.d. random points will be recognised as non-hyperuniform.

We use the notation

$$C(\mathbf{x}, \phi) = \{\mathbf{y} \in \mathbb{S}^d \mid \langle \mathbf{x}, \mathbf{y} \rangle > \cos \phi\}$$

for the spherical cap with center $\mathbf{x}$ and opening angle ϕ.

Definition 1 (Number variance)**.** *Let $\mathscr{X}_N$ be a point process on the sphere $\mathbb{S}^d$ sampling N points. The* number variance *of $\mathscr{X}_N$ for caps of opening angle ϕ is given by*

$$V(\mathscr{X}_N, \phi) := \mathbb{V}\mathscr{X}_N(C(\cdot, \phi)) := \mathbb{E}\left(\mathscr{X}_N(C(\cdot, \phi))^2\right) - \left(\mathbb{E}\mathscr{X}_N(C(\cdot, \phi))\right)^2. \tag{1}$$

If the process $\mathscr{X}_N$ is rotation invariant, the implicit integration with respect to the center of the cap $C(\cdot, \phi)$ can be omitted.

Throughout the paper we write $\sigma(C(\phi))$ for the normalised surface area of the cap.

Definition 2 (Hyperuniformity)**.** *Let $\mathscr{X}_N$ be a point process on the sphere $\mathbb{S}^d$ sampling N points. The process $(\mathscr{X}_N)$ is called*

- ***hyperuniform for large caps** if*

$$V(\mathscr{X}_N, \phi) = o(N) \quad \text{as } N \to \infty \tag{2}$$

for all $\phi \in (0, \frac{\pi}{2})$;

- ***hyperuniform for small caps*** *if*

$$V(\mathscr{X}_N, \phi_N) = o\left(N\sigma(C(\phi_N))\right) \quad \text{as } N \to \infty \tag{3}$$

and all sequences $(\phi_N)_{N\in\mathbb{N}}$ *such that*
  (1) $\lim_{N\to\infty} \phi_N = 0$
  (2) $\lim_{N\to\infty} N\sigma(C(\phi_N)) = \infty$, *which is equivalent to* $\phi_N N^{\frac{1}{d}} \to \infty$ *for* $N \to \infty$.

- ***hyperuniform for caps at threshold order*** *if*

$$\limsup_{N\to\infty} V(\mathscr{X}_N, tN^{-\frac{1}{d}}) = \mathcal{O}(t^{d-1}) \quad \text{as } t \to \infty. \tag{4}$$

The $\mathcal{O}(t^{d-1})$ *in* (4) *could be replaced by the less strict* $o(t^d)$ *in a more general setting.*

Remark 1. *Notice that the definition for processes* $\mathscr{X}_N$ *includes the case of deterministically constructed point sets by just concentrating the measure on the specified point set* X_N. *The variances used in the definition are then obtained by integrating* $(\#(X_N \cap C(\mathbf{x}, \phi)) - N\sigma(C(\mathbf{x}, \phi)))^2$ *with respect to* $\mathbf{x}$.

Remark 2. *The definition of hyperuniformity is designed so that the number variance of a hyperuniform point set in any of the three regimes is of smaller order than the corresponding number variance of i.i.d. random points. This singles out sequences of i.i.d. random point sets as non-hyperuniform.*

In [4] it has been shown that hyperuniformity in any of the three regimes implies asymptotic uniform distribution. Furthermore, it has been shown that sequences of spherical t-designs of minimal growth order (see [3]), as well as QMC-designs (see [6]), and point sets maximising the sum of mutual distances (see [7, 8]) are hyperuniform.

In [5] it has been shown that the spherical ensemble on $\mathbb{S}^2$ (see [1]), the harmonic ensemble on $\mathbb{S}^d$ (see [2]), as well as jittered sampling processes are hyperuniform for all three regimes. Furthermore, it is shown that the jittered sampling process is a determinantal process.

References

[1] K. Alishahi and M. Zamani, *The spherical ensemble and uniform distribution of points on the sphere*, Electron. J. Probab. **20** (2015), no. 23, 27.

[2] C. Beltrán, J. Marzo, and J. Ortega-Cerdà, *Energy and discrepancy of rotationally invariant determinantal point processes in high dimensional spheres*, J. Complexity **37** (2016), 76–109.

[3] A. V. Bondarenko, D. Radchenko, and M. S. Viazovska, *Optimal asymptotic bounds for spherical designs*, Ann. of Math. (2) **178** (2013), no. 2, 443–452.

[4] J. S. Brauchart, P. J. Grabner, and W. B. Kusner, *Hyperuniform point sets on the sphere: deterministic aspects*, Constr. Approx. (2019), to appear.

[5] J. S. Brauchart, P. J. Grabner, W. B. Kusner, and J. Ziefle, *Hyperuniform point sets on the sphere: probabilistic aspects*, `https://arxiv.org/abs/1809.02645`, 2018.

[6] J. S. Brauchart, E. B. Saff, I. H. Sloan, and R. S. Womersley, *QMC designs: optimal order Quasi Monte Carlo integration schemes on the sphere*, Math. Comp. **83** (2014), no. 290, 2821–2851.

[7] K. B. Stolarsky, *Sums of distances between points on a sphere*, Proc. Amer. Math. Soc. **35** (1972), 547–549.
[8] ———, *Sums of distances between points on a sphere. II*, Proc. Amer. Math. Soc. **41** (1973), 575–582.
[9] S. Torquato and F. H. Stillinger, *Local density fluctuations, hyperuniformity, and order metrics*, Phys. Rev. E **68** (2003), no. 4, 041113.

Finite crystallization in the hexagonal lattice for ionic dimers

Leonard Kreutz
(joint work with Manuel Friedrich)

The *crystallization problem* (see [1] for a review) is the challenge to prove rigorously that global minimizers of certain configurational energies arrange in periodic structures. We contribute to this fundamental mathematical question by investigating particle systems consisting of two different atomic types, also called *dimers*.

We follow the framework of molecular mechanics of configurational energy minimization. Identifying configurations of n particles with their respective positions $\{x_1, \dots, x_n\} \subset \mathbb{R}^2$ and additionally with their types $\{q_1, \dots, q_n\} \in \{-1, +1\}^n$ our goal is to determine global minimizers of a corresponding interaction energy of the form

$$\mathcal{E}((x_1, q_1), \dots, (x_n, q_n)) = \frac{1}{2} \sum_{\substack{i \neq j \\ q_i \neq q_j}} V_{\mathrm{a}}(|x_i - x_j|) + \frac{1}{2} \sum_{\substack{i \neq j \\ q_i = q_j}} V_{\mathrm{r}}(|x_i - x_j|).$$

The potentials V_{a} and V_{r} are short ranged attractive repulsive and respectively short ranged purely repulsive potentials. Under suitable assumptions on the attractive and the repulsive potential we show that each global minimizers of the configurational energy is essentially a connected subset of the hexagonal lattice with the two atomic types alternating, see e.g. Fig 2. However for small n other

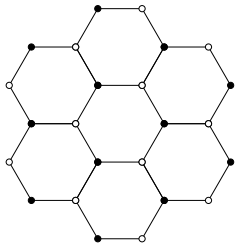

Figure 2. A hexagonal groundstate

polygons may occur in the bond graph of minimizers and thus fine geometric characterizations of minimizers need to be employed in order to prove the crystallization result for n big enough. Next we are able to characterize the minimal

energy explicitly. It coincides with the one in [3] where the crystallization of carbon structures in the plane has been investigated. Finally we characterize the *net charge*, that is the (signed) difference of the number of the two atomic types. Analysing the deviation of configurations from the hexagonal *Wulff shape* [2], we prove that for ground states consisting of n particles the net charge is at most of the order $O(n^{1/4})$ where the scaling is sharp. All the presented results are contained in [4].

References

[1] X. Blanc, M. Lewin, *The crystallization conjecture: a review*, EMS Surveys in Mathematical Sciences **2** (2015), 255–306.

[2] E. Davoli, P. Piovano, U. Stefanelli, *Wulff Shape emergence in grahene*, Mathematical Models and Methods in Applied Sciences **26** (2016), 12:2277–2310.

[3] E. Mainini, U. Stefanelli, *Crystallization in carbon nanostructures*, Communications in Mathematical Physics **328** (2014), 545–571.

[4] M. Friedrich, L. Kreutz, *Crystallization in the hexagonal lattice for ionic dimers*, submitted.

Energy minimization of 2D incommensurate heterostructures

Mitchell Luskin

(joint work with Paul Cazeaux, Daniel Massatt)

We derive and analyze a novel approach for modeling and computing the mechanical relaxation of incommensurate 2D heterostructures. Our approach parametrizes the relaxation pattern by the compact local configuration space rather than real space, thus bypassing the need for the standard supercell approximation and giving a true aperiodic atomistic configuration. Our model extends the computationally accessible regime of weakly coupled bilayers with similar orientations or lattice spacing, for example materials with a small relative twist where the widely studied large-scale moire patterns arise. Our model also makes possible the simulation of multi-layers for which no interlayer empirical atomistic potential exists, such as those composed of MoS2 layers, and more generally makes possible the simulation of the relaxation of multi-layer heterostructures for which a planar moire pattern does not exist.

References

[1] S. Carr, D. Massatt, S. B. Torrisi, P. Cazeaux, M. Luskin, and E. Kaxiras. Relaxation and Domain Formation in Incommensurate 2D Heterostructures. *Physical Review B*, to appear.

[2] P. Cazeaux, M. Luskin, and D. Massatt. Energy minimization of 2D incommensurate heterostructures. *ArXiv e-prints 1806.10395*, June 2018.

Atomistic potentials and the Cauchy-Born rule for carbon nanotubes

Edoardo Mainini
(joint work with Manuel Friedrich, Paolo Piovano, Ulisse Stefanelli)

In the framework of Molecular Mechanics, we describe the interaction of n particles $x_1, \dots, x_n$ in $\mathbb{R}^3$ by means of classical atomistic potentials including two- and three-body terms, namely

$$E(x_1, \dots, x_n) = \frac{1}{2} \sum_{ij \in NN} V_2(|x_i - x_j|) + \frac{1}{2} \sum_{ij,jk \in NN} V_3(\theta_{ijk}).$$

Here, V_2 is an attractive-repulsive potential of Lennard-Jones type that measures bond lengths, whereas V_3 is an angle potential that favors bond angles θ_{ijk} of 120 degrees, in order to describe sp^2 covalent bonds of carbon atoms in graphene. Only distinct nearest-neighbor (NN) interactions are taken into account.

A carbon nanotube is an atom-thick cylindrical layer of carbon atoms, which can be viewed as the result of rolling-up a graphene sheet. We show that specific rolled-up hexagonal configurations, made by n particles lying on the surface of a cylinder and exhibiting periodicity along the axis direction, provide local minimality for the energy E among spatial configurations with the same number of particles. Moreover, such local minimizers are shown to be obtained by optimizing among suitable one-parameter families of objective configurations.

We also consider nanotubes under moderate stretching. In presence of applied axial tension, we still show existence of a periodic local minimizer so that the atoms follow the macroscopic deformation. This provides a justification of the elastic behaviour of carbon nanotubes in the small traction regime.

Crucial steps of the proof are a careful choice of the energy decomposition in basic cell contributions, a detailed estimate of the behavior of the energy under local symmetrization procedures and the analysis of lower dimensional problems as detailed in [1], [2], [3].

References

[1] E. Mainini, H. Murakawa, P. Piovano, U. Stefanelli, *Carbon-nanotube geometries: analytical and numerical results*, Discrete Contin. dyn. Syst. Series S **10** (2017), 141–160.

[2] E. Mainini, H. Murakawa, P. Piovano, U. Stefanelli, *Carbon-nanotube geometries as optimal configurations*, Multiscale Model. Simul. **15** (2017), 1448–1471.

[3] M. Friedrich, E. Mainini, P. Piovano, U. Stefanelli, *Characterization of optimal carbon nanotubes under stretching and validation of the Cauchy-Born rule*, Arch. Ration. Mech. Anal., DOI: 10.1007/s00205-018-1284-7.

Collective dynamics through body attitude coordination

Sara Merino-Aceituno
(joint work with Pierre Degond, Amic Frouvelle, Ariane Trescases)

We present a new model for multi-agent dynamics where each agent is described by its position and body attitude: agents travel at a constant speed in a given direction and their body can rotate around it adopting different configurations. Agents try to coordinate their body attitudes with the ones of their neighbours. This model is inspired by the Vicsek model. The body position is described as a rotation, i.e, once fixed a reference frame the body position is given as a rotation of this frame. One of the vectors of the reference frame gives the direction of motion while the other two give the relative position of the body with respect to the direction of motion.

The goal of this talk will be to present this new flocking model, its relevance and the derivation of the macroscopic equations from the particle dynamics. Two approaches are considered: one in which rotations are described using rotation matrices [1] and another using unitary quaternions [2]. Modelling is more natural using rotation matrices but from a computational point-of-view, quaternions give better performance and less memory usage.

Specifically, we present an individual based model for body attitude coordination given by the evolution over time of $(X_k, A_k)_{k=1,\dots,N}$ of N agents, where $X_k \in \mathbb{R}^3$ is the position of agent k and $A_k \in SO(3)$ is a rotation matrix giving its body attitude. The evolution of the system is given by the following equations:

$$d\mathbf{X_k}(t) = v_0 A_k(t)\mathbf{e_1}dt, \tag{1}$$

$$dA_k(t) = P_{T_{A_k}} \circ \left[\nu \mathrm{PD}(M_k)dt + 2\sqrt{D}dW_t^k\right], \tag{2}$$

where the Stochastic Differential Equation is in Stratonovich sense; W_t^k is the Brownian motion in the space of squared matrices; M_k is defined as

$$M_k(t) := \frac{1}{N}\sum_{i=1}^{N} K(|\mathbf{X}_i(t) - \mathbf{X_k}(t)|)A_i(t), \tag{3}$$

where K is a positive interaction kernel; ν, v_0 and D are positive constants; $\mathbf{e_1}$ is a vector; and P_{T_A} is the projection in $SO(3)$ to the tangent space to A. The term $\mathrm{PD}(M)$ denotes the orthogonal matrix obtained from the polar decomposition of M. The equivalent model can be written using unitary quaternions and nematic alignment. The macroscopic equations are complex and different from those of the Vicsek model (where the particles only align and body attitude is not considered).

References

[1] Degond, Pierre and Frouvelle, Amic and Merino-Aceituno, Sara, *A new flocking model through body attitude coordination*, Math. Models Methods Appl. Sci. **27** (2017), 1005–1049.

[2] Degond, Pierre and Frouvelle, Amic and Merino-Aceituno, Sara and Trescases, Ariane, *Quaternions in collective dynamics*, Multiscale Modeling & Simulation, **16** (2018), 28–77.

Plastically deformed solids in continuum approximation

Franz Merkl
(joint work with Roland Bauerschmidt, Diana Conache, Markus Heydenreich, Silke Rolles)

We analyze a toy model for the statistical mechanics of dislocation lines in 3 dimensions on a mesoscopic scale in the spirit of the Fröhlich-Spencer analysis of the Villain model. The goal is to understand spontaneous breaking of linearized rotational symmetry in the presence of dislocation lines.

Features of the model:

- model within *equilibrium statistical mechanics*: no dynamics
- positive, *small temperature*
- *mesoscopic* scale: no individual atoms in the model: local displacement modeled by a smooth field
- *linear elasticity theory* used for elastic energy
- just for simplicity: isotropy assumption for quadratic elastic energy
- *UV cutoff:* dislocation lines supported on edges of a mesoscopic lattice with edge set Λ, vertex set V_Λ, not to be confused with an atomic lattice, but smeared out with a form function φ with small support,
- *Burgers vectors* take values in a *microscopic* lattice Γ, not to be confused with Λ.
- *linearized rotational symmetry spontaneously broken*

Basic objects in the model:

- a smooth field $w : \mathbb{R}^3 \to \mathbb{R}^{3\times 3}$. Interpretation in the absence of dislocations: Gradient field $w = \nabla u$ of the displacement field $u : \mathbb{R}^3 \to \mathbb{R}^3$
- Burgers vector density $b_{ijk} = \partial_i w_{jk} - \partial_j w_{ik}$, for short $b = d_1 w$.
- total energy $H(w) = H_{\mathrm{el}}(w) + H_{\mathrm{disl}}(d_1 w)$
- symmetry and lower bound assumption: $H_{\mathrm{disl}}(b) = H_{\mathrm{disl}}(-b) \geq \mathrm{const}\|b\|_1$
- locality assumption: $H_{\mathrm{disl}}(b_1 + b_2) = H_{\mathrm{disl}}(b_1) + H_{\mathrm{disl}}(b_2)$ for $\operatorname{supp} b_1 \cap \operatorname{supp} b_2 = \emptyset$

Discrete dislocation lines: Consider a finite subset of edges $E \subset \Lambda$, set of vertices V.

- Just for bookkeeping purposes, associate a counting direction to every edge, encoded in a signed incidence matrix $\sigma : V \times E \to \{0, \pm 1\}$.
- Burgers vector field modeled by $I : E \to \Gamma$ with the Kirchhoff node rule constraint $\sum_{e\in E} \sigma_{ve} I_e = 0$ for all $v \in V$. $\mathcal{I} = \mathcal{I}(E) \subset \Gamma^E$: set of Burgers vector fields with this constraint.
- associated vector valued current as a signed vector valued measure: $J_{jk}(I) = \sum_{e\in E} (n_e)_j (I_e)_k \lambda_e$, $j, k \in \{1, 2, 3\}$), where λ_e denotes the 1-dim Lebesgue measure on e and n_e the unit vector in counting direction of e.

- Burgers vector field obtained by convolution with form function φ:

$$b_{ijk} = \sum_{l=1}^{3} \epsilon_{ijl} \varphi * J_{lk}(I)$$

Linear model for elastic energy: Quadratic elastic energy H_{el} with an isotropic quadratic elastic energy density:

$$H_{\mathrm{el}}(w) = \int_{\mathbb{R}^3} F(w(x) + w(x)^t)\, dx, \quad F(U) = \frac{\lambda}{2}(\operatorname{Tr} U)^2 + \mu \|U\|_2^2$$

Thermal measure:

- Minimization over elastic degrees of freedom (corresponding to spin waves in the Villain model):

$$H_{\mathrm{el}}^*(I) = \inf_{\substack{w \in C_c^\infty(\mathbb{R}^3, \mathbb{R}^{3\times 3}): \\ d_1 w = b(I)}} H_{\mathrm{el}}(w)$$

- Partition sum and thermal measure:

$$Z_\beta = \sum_{I \in \mathcal{I}} e^{-\beta(H_{\mathrm{el}}^*(I) + H_{\mathrm{disl}}(I))}, \quad P_\beta = \frac{1}{Z_\beta} \sum_{I \in \mathcal{I}} e^{-\beta(H_{\mathrm{el}}^*(I) + H_{\mathrm{disl}}(I))} \delta_I$$

Linearized rotational symmetry: There are null directions in the energy functionals corresponding to linearized rotational symmetry: $H_{\mathrm{el}}(w) = H_{\mathrm{el}}(w + w_{\mathrm{const}})$ and $d_1 w = d_1(w + w_{\mathrm{const}})$ for constant antisymmetric $w_{\mathrm{const}} \in \mathbb{R}^{3\times 3}$.
Boundary condition "w compactly supported" breaks this linearized rotational symmetry.

Lemma (Minimizer in L^2 of the elastic energy): For any $I \in \mathcal{I}$, there is a bounded smooth function $w^*(\cdot, I) \in L^2(\mathbb{R}^3, \mathbb{R}^{3\times 3})$ such that for any sequence $(w^n)_{n\in\mathbb{N}}$ in $C_c^\infty(\mathbb{R}^3, \mathbb{R}^{3\times 3})$ with $d_1 w^n = b(I)$ for all $n \in \mathbb{N}$ and $\lim_{n\to\infty} H_{\mathrm{el}}(w^n) = H_{\mathrm{el}}^*(I)$ we have $\lim_{n\to\infty} \|w^n - w^*(\cdot, I)\|_2 = 0$.

Theorem (Spontaneous breaking of linearized rotational symmetry): There is a constant $c_1 > 0$ such that for all large β and for all $t \in \mathbb{R}$,

$$\inf_{E \Subset \Lambda} \inf_{x,y \in \mathbb{R}^3} \min_{i,j\in[3]} E_{P_\beta}\left[e^{it(w_{ij}^*(x,I) - w_{ij}^*(y,I))}\right] \geq \exp\Big\{ -\frac{t^2}{2}\, e^{-c_1\beta}\Big\},$$

and consequently

$$\sup_{E \Subset \Lambda} \sup_{x,y \in \mathbb{R}^3} \max_{i,j\in[3]} \operatorname{Var}_{P_\beta}\left(w_{ij}^*(x,I) - w_{ij}^*(y,I)\right) \leq e^{-c_1\beta}.$$

Interpretation: Breaking of linearized rotational symmetry by boundary conditions remains as a *spontaneously broken symmetry* in the thermodynamic limit.

Steps for the proof:

- Minimization of the elastic energy in a suitable Sobolev space.

In the spirit of the analysis of the Villain model by Fröhlich and Spencer, the next steps are:

- *Sine-Gordon transformation* (introduction of an auxiliary Gaussian field) for the elastic energy,
- *Cluster expansion* of the free energy
- Bounding the observable $w^*(x, I)$ with a variant of the *dipole expansion* in magnetostatics

References

[1] R. Bauerschmidt, D. Conache, M. Heydenreich, F. Merkl, S. Rolles, *Dislocation lines in three-dimensional solids at low temperature.* In preparation, (2018).

Equilibrium Measures for Nonlocal Interaction Energies: The Role of Anisotropy

Maria Giovanna Mora

(joint work with J.A. Carrillo, J. Mateu, L. Rondi, L. Scardia, J. Verdera)

In this talk I discussed the minimization problem for the nonlocal energy

$$I_\alpha(\mu) = \iint_{\mathbb{R}^2\times\mathbb{R}^2} W_\alpha(x-y)\,d\mu(x)\,d\mu(y) + \int_{\mathbb{R}^2} |x|^2\,d\mu(x) \tag{1}$$

defined on the class $\mathcal{P}(\mathbb{R}^2)$ of probability measures, where the interaction potential W_α is given by

$$W_\alpha(x_1,x_2) = -\frac{1}{2}\log(x_1^2+x_2^2) + \alpha\frac{x_1^2}{x_1^2+x_2^2}, \qquad x=(x_1,x_2)\in\mathbb{R}^2,$$

and $\alpha\in\mathbb{R}$. Here the parameter α has the role of *tuning* the strength of the anisotropic component of W_α, making it more or less prominent.

The energy (1) arises as the Γ-limit of discrete interaction energies of systems of n particles, as n tends to infinity. More precisely, I_α is the Γ-limit of F_n/n^2, where

$$F_n(x^1,\dots,x^n) = \sum_{i=1}^n\sum_{j\neq i} W_\alpha(x^i-x^j) + n\sum_{i=1}^n |x^i|^2, \qquad \{x^i\}\subset\mathbb{R}^2,$$

with respect to the weak* convergence of the empirical measures $\frac{1}{n}\sum_i \delta_{x^i}$. Therefore, I_α is the leading order or *mean-field* behaviour of the Hamiltonian F_n, and the minimizers of I_α represent the mean-field description of the minimizers of F_n, namely the equilibrium configurations at the mesoscale.

In the particular case where the anisotropy is *switched off*, namely for $\alpha=0$, the minimizer is radial, and is given by the celebrated circle law $\mu_0 := \frac{1}{\pi}\chi_{B_1(0)}$, the normalized characteristic function of the unit disk. This result is now classical and has been proved in a variety of contexts, from Fekete sets to orthogonal

polynomials, from random matrices to Ginzburg-Landau vortices and Coulomb gases (see, e.g., [1, 4]).

In the case $\alpha = 1$, the energy I_1 models interactions between edge dislocations of the same sign. The minimizers of I_1 were since long conjectured to be vertical walls of dislocations, and this has been confirmed only very recently, in [3], where the authors proved that the only minimizer of I_1 is the semi-circle law

$$\mu_1 := \frac{1}{\pi}\delta_0 \otimes \sqrt{2 - x_2^2}\, \mathcal{H}^1 \llcorner (-\sqrt{2}, \sqrt{2}) \tag{2}$$

on the vertical axis.

In this talk I showed that the minimizer of I_α can be explicitly characterized for every $\alpha \in \mathbb{R}$. In particular, it turns out that the values $\alpha = \pm 1$ are *critical* values of the parameter, corresponding to *maximal anisotropy*, at which an abrupt change in the dimension of the support of the minimizer occurs. Indeed, for $\alpha \in (-1, 1)$ we prove that the unique minimizer of I_α is given by

$$\mu_\alpha := \frac{1}{\pi\sqrt{1-\alpha^2}} \chi_{\Omega(\sqrt{1-\alpha}, \sqrt{1+\alpha})},$$

where

$$\Omega(\sqrt{1-\alpha}, \sqrt{1+\alpha}) := \left\{ x \in \mathbb{R}^2 : \ \frac{x_1^2}{1-\alpha} + \frac{x_2^2}{1+\alpha} < 1 \right\},$$

that is, the normalized characteristic function of the region surrounded by an ellipse. On the other hand, we show that for every $\alpha \geq 1$ the only minimizer of I_α is the semi-circle law μ_1 on the vertical axis, while for $\alpha \leq -1$ it is the semi-circle law on the horizontal axis.

The result for $\alpha > 1$ can be obtained by a simple comparison argument, and for $\alpha < 0$ by symmetry. For $0 \leq \alpha \leq 1$ we prove the minimality of μ_α by showing that μ_α satisfies the Euler-Lagrange conditions

$$(W_\alpha * \mu_\alpha)(x) + \frac{|x|^2}{2} = C_\alpha \quad \text{for every } x \in \Omega(\sqrt{1-\alpha}, \sqrt{1+\alpha}), \tag{3}$$

$$(W_\alpha * \mu_\alpha)(x) + \frac{|x|^2}{2} \geq C_\alpha \quad \text{for every } x \in \mathbb{R}^2, \tag{4}$$

for some constant C_α. Those conditions are sufficient for minimality, since we show that the energy I_α is strictly convex for $-1 \leq \alpha \leq 1$.

To prove (3)–(4) we evaluate the convolution of the kernel W_α with the characteristic function of the domain $\Omega(a, b)$ enclosed by a general ellipse of semi-axes a and b. The logarithmic potential $W_0 * \chi_{\Omega(a,b)}$ has been computed before in the context of fluid dynamics [2]. The challenge is computing the anisotropic part of the potential function $W_\alpha * \chi_{\Omega(a,b)}$. The key observation is that a formula for the anisotropic potential inside the ellipse can be deduced by differentiating the logarithmic potential $W_0 * \chi_{\Omega(a,b)}$ with respect to one of the semi-axes. With an explicit formula for $W_\alpha * \chi_{\Omega(a,b)}$ inside $\Omega(a, b)$ at hand, condition (3) can be directly checked. To show (4) we apply an argument based on the maximum principle for harmonic functions.

It is worth emphasizing the special role played by ellipses. On the one hand, in fluid mechanics they provide one of the few explicit solutions of the incompressible Euler equations (Kirchhoff ellipses). On the other hand, the characteristic function of the elliptical domains $\Omega(a,b)$ is one of the few measures μ for which the convolution potential $W_\alpha * \mu$ can be explicitly computed.

References

[1] O. Frostman, *Potentiel d'équilibre et capacité des ensembles avec quelques applications à la théorie des fonctions*, Meddel. Lunds Univ. Mat. Sem., 3:1–118, 1935.

[2] G. Kirchhoff, *Vorlesungen über mathematische Physik*, Teubner, Leipzig, 1874.

[3] M.G. Mora, L. Rondi, and L. Scardia, *The equilibrium measure for a nonlocal dislocation energy*, Comm. Pure Appl. Math., to appear.

[4] E.B. Saff and V. Totik, *Logarithmic potentials with external fields*, Springer-Verlag, Berlin, 1997.

Microscopic validation of a variational model for epitaxially-strained crystalline films

Paolo Piovano

(joint work with Leonard Kreutz)

A discrete model for crystalline films deposited on substrates in the presence of a mismatch between the parameters of the film and the substrate crystalline lattices is introduced, and a discrete-to-continuum passage is performed by Γ-convergence. As the obtained Γ-limit is in agreement with literature continuum models [2, 3, 4], the presented analysis represents also a microscopical justification of such models.

The discrete variational model is characterized by an energy denoted by E^ε that depends on triples (h,y,u) of functions defined with respect to a reference lattice $\mathcal{L}_\varepsilon$, where $\varepsilon>0$ is a rescaling parameter. More precisely, we choose the triangular lattice $\mathcal{L}_\varepsilon := \{(i\mathbf{a}+j\mathbf{b}+k\mathbf{c})\varepsilon/4 : i,j\in\mathbb{Z}, k=0,1\}$ with $\mathbf{a}:=(5\sqrt{3},0)$, $\mathbf{b}:=(\sqrt{3},4)$, and $\mathbf{c}:=(3\sqrt{3},2)$, and the functions h,y,u represent the film heights, the bulk deformations, and the bulk displacements, respectively. We say that $h:\varepsilon\sqrt{3}/2(\mathbb{Z}+\frac{1}{2})\cap(0,L)\to\mathbb{R}_+$, for a fixed $L>0$, is a film *discrete height* if

$$h\left(\frac{\sqrt{3}}{2}\varepsilon\left(i+\frac{1}{2}\right)\right)\in\begin{cases}\frac{\varepsilon}{2}+\varepsilon\mathbb{N} & i \text{ even},\\ \varepsilon\mathbb{N} & i \text{ odd},\end{cases}$$

and we identify each discrete height h with a properly characterized lower-semicontinuous piecewise constant interpolation over the interval $(0,L)$. Thus, the set $\Omega_h^+ := \big\{(x_1,x_2)\in\mathbb{R}^2 : 0<x_1<L, 0<x_2<h(x_1)\big\}$ represents the region occupied by films with height h, while $\Omega^-=\big\{(x_1,x_2)\in\mathbb{R}^2 : 0<x_1<L, -R<x_2\le 0\big\}$, for a fixed $R>0$, is the substrate region. Furthermore, we call *discrete deformation* every function $y:\mathcal{L}_\varepsilon(\Omega_h)\to\mathbb{R}^2$ where $\mathcal{L}_\varepsilon(\Omega_h):=\mathcal{L}_\varepsilon\cap\Omega_h$ with $\Omega_h:=\Omega_h^+\cup\Omega^-$, and we assume that each deformation y is *orientation-preserving* (see [1]), i.e.,

$$\det\big(y(\tilde{x})-y(x), y(\bar{x})-y(x)\big)\det(\tilde{x}-x,\bar{x}-x)\ge 0$$

for every mutual nearest neighbors $x, \tilde{x}, \bar{x} \in \mathcal{L}_\varepsilon(\Omega_h)$. Given a discrete deformation y we refer to every $u : \mathcal{L}_\varepsilon(\Omega_h) \to \mathbb{R}^2$ defined by $u(x) = \varepsilon^{-1/2}(y(x) - (Rx + b))$ for some rotation $R \in SO(2)$ and $b \in \mathbb{R}^2$, as a *discrete displacement* associated to y.

The ε-rescaled energy E_ε is defined on *discrete triples* (h, y, u), i.e., triples (h, y, u) where h is a discrete height, y a discrete deformation, and u a discrete displacement associated to y, by

$$E_\varepsilon(h, y, u) := \sum_{x \in \mathcal{L}_\varepsilon(\Omega_h)} \sum_{\tilde{x} \in \mathcal{N}_\varepsilon(x)} \varepsilon V_x^\varepsilon \left(\frac{|y(x) - y(\tilde{x})|}{\varepsilon} \right) + \sum_{x \in \mathcal{L}_\varepsilon(\Omega_h)} \varepsilon \gamma(x)(6 - \#\mathcal{N}_\varepsilon(x)),$$

where $\mathcal{N}_\varepsilon(x) = \left\{ \tilde{x} \in \mathcal{L}_\varepsilon(\Omega_h) \setminus \{x\} : |\tilde{x} - x| \le \varepsilon \text{ or } |\tilde{x} \pm L\mathbf{a}/(5\sqrt{3}) - x| \le \varepsilon \right\}$ denotes the set of nearest neighbors (with L-periodic condition) of $x \in \mathcal{L}_\varepsilon(\Omega_h)$,

$$V_x^\varepsilon(r) = \begin{cases} \frac{K_f}{2}(r - \lambda_\varepsilon)^2 & \text{if } x \in \Omega_h^+, \\ \frac{K_s}{2}(r-1)^2 & \text{if } x \in \Omega^-, \end{cases} \quad \text{and} \quad \gamma(x) := \begin{cases} \gamma_f & \text{if } x \in \Omega_h^+, \\ \gamma_s & \text{if } x \in \Omega^-, \end{cases}$$

for constants $\gamma_f, \gamma_s, K_f, K_s > 0$, and the parameter $\lambda_\varepsilon > 0$ represents the optimal bonding distance for film atoms. Furthermore, we impose a *ε-volume constraint* on discrete heights h, i.e., $\|h\|_{L^1} = V_\varepsilon$ for $V_\varepsilon \in \varepsilon^2\sqrt{3}/2\mathbb{N}$ chosen so that $V_\varepsilon \to V > 0$.

In order to perform a discrete-to-continuum analysis it is convenient to embed the discrete triples (h, y, u) to the larger configurational space

$$X := \left\{ (h, y, u) : \ h \text{ is l.s.c. with } \mathrm{Var} h < +\infty, \text{ and } y, u \in L^2_{\mathrm{loc}}(\Omega_h; \mathbb{R}^2) \right\}$$

by identifying y and u with properly defined piecewise affine interpolations in Ω_h, and by extending E_ε to be $+\infty$ on non-discrete triples in X. We consider in X the metrizable topology τ_X associated to the following notion of convergence: $(h_\varepsilon, y_\varepsilon, u_\varepsilon) \to (h, y, u) \in X$ if $y_\varepsilon \to y$ and $u_\varepsilon \to u$ in $L^2_{\mathrm{loc}}(\Omega_h; \mathbb{R}^2)$, and $\mathbb{R}^2 \setminus \Omega_{h_\varepsilon}$ converge to $\mathbb{R}^2 \setminus \Omega_h$ with respect to the Hausdorff-distance. Furthermore, we work in the *small mismatch regime* by assuming that $\varepsilon^{-\frac{1}{2}}(\lambda_\varepsilon - 1) \to \eta$ for some $\eta \in \mathbb{R}$.

As a first results obtained by regrouping the elastic energy in *triangular-cell energies* and by establishing a discrete rigidity estimate, it turns out that energy equi-bounded sequences, i.e., sequences $(h_\varepsilon, y_\varepsilon, u_\varepsilon)$ such that $\sup\{E^\varepsilon(h_\varepsilon, y_\varepsilon, u_\varepsilon) : \varepsilon > 0\} < \infty$, are pre-compact (apart from redefining the displacements associated to y_ε) in X. The second presented result consists in the Γ-convergence as $\varepsilon \to 0$ with respect to τ_X of the energies E_ε to the continuum energy $\mathcal{E}$ defined in X by

$$\mathcal{E}(y, u, h) = \begin{cases} \mathcal{F}(y, u, h) & \text{if } \|h\|_{L^1} = V \text{ and } y = Rx + b \text{ for some } (R, b) \in SO(2) \times \mathbb{R}^2 \\ +\infty & \text{otherwise,} \end{cases}$$

where, if Γ_h is the graph of h and Γ_h^{cut} its cut portions, $\mathcal{F}(y, u, h)$ is given by

$$\mathcal{F}(y, u, h) = \int_{\Omega_h} W_0(x_2, Eu(x))\mathrm{d}x + \int_{\Gamma_h \setminus \Gamma_h^{cut}} \varphi(x_2)\psi(\nu)\, d\mathcal{H}^1 + 2\int_{\Gamma_h^{cut}} \gamma_f \psi(\nu)\, d\mathcal{H}^1$$

where $W_0(x_2, A) := \frac{16}{\sqrt{3}} K(x_2) \left(|A - E_0(x_2, y)|^2 + \frac{1}{2} Tr^2(A - E_0(x_2, y)) \right)$ for

$$K(x_2) := \begin{cases} K_f & \text{if } x_2 > 0, \\ K_s & \text{if } x_2 \leq 0, \end{cases} \quad E_0(x_2, y) := \begin{cases} \eta \nabla y & \text{if } x_2 > 0, \\ 0 & \text{if } x_2 \leq 0, \end{cases} \quad \varphi(x_2) := \begin{cases} \gamma_f & \text{if } x_2 > 0, \\ \gamma_{\mathrm{f}} \wedge \gamma_{\mathrm{s}} & \text{if } x_2 = 0, \end{cases}$$

and $\psi(\nu) := 2\sqrt{3}/3 \left(|\nu_2| + 1/2 \left| \sqrt{3}\nu_1 - \nu_2 \right| + 1/2 \left| \sqrt{3}\nu_1 + \nu_2 \right| \right)$. Notice that $\mathcal{F}$ is of the same type as the model in [4] and its surface-density form allows to distinguish the *wetting* from the *dewetting regime* as in [2, 3]. Moreover, it displays a mismatch strain E_0 that directly depends on the limit η of the ε-rescaled lattice mismatches.

References

[1] A. Braides, M. Solci, E. Vitali, *A derivation of linear elastic energies from pair-interaction atomistic systems*, Netw. Heterog. Media **2** (2007), 551–567.

[2] E. Davoli, P. Piovano, *Derivation of a heteroepitaxial thin-film model*, Submitted (2018).

[3] I. Fonseca, N. Fusco, G. Leoni, M. Morini, *Equilibrium configurations of epitaxially strained crystalline films: existence and regularity results*, Arch. Ration. Mech. Anal. **186** (2007), 477–537.

[4] B. J. Spencer, J. Tersoff, *Equilibrium shapes and properties of epitaxially strained islands*, Phys. Rev. Lett. **79** (1997), 4858.

The emergence of structure as fluids freeze, and analogous phase transitions

Charles Radin

For background a review was given of thermodynamic pressure/temperature phase diagrams of simple matter, and the role of statistical mechanics as a bridge between the many position/velocity variables of constituent molecules and the few variables labeling the states of bulk matter in thermodynamic equilibrium. The example of the hard sphere model was emphasized, simulations of which exhibit sharp melting and freezing transitions between (crystalline) solid and (disordered) fluid phases, without any attraction in the interaction.

It is an old unsolved problem to prove the existence of a thermodynamic fluid/solid phase transition using statistical mechanics, for instance using the hard sphere model. We considered a different, dynamical approach using nucleation theory, which is supposed to model how molecules in a disordered fluid initiate rearrangement into a crystalline solid, upon 'supercooling'. The probabilistic theory is supposed to predict the existence of 'critical size' clusters of molecules; crystalline molecular clusters which are smaller in size generally shrink, larger ones generally grow.

Classical nucleation theory has not yet been a reliable guide to the rate of production and growth of critical nuclei, presumably because it is experimentally difficult to directly study the nucleation process physically. Therefore we discussed two substitute regimes, with analogues of 'ordered structure emerging from disorder' in the above traditional sense.

The first was a recent physical experiment, joint work with F. Rietz, H. Swinney and M. Shroeter, on granular matter ('bulk sand') [1, 2], in which careful, gentle

cyclic shear was found to drive the grains in a disordered bed of sand into critical crystalline clusters of about 10 grains, which then turn the bed into a polycrystalline state. In other words, given an appropriate dynamics sand nucleates into a crystalline form. There is ongoing development of a statistical theory of bulk sand initiated in 1989 by Edwards and Oakshott [3], but in it the grains are static. The recent experiment shows precisely how to introduce a physical dynamics, using shear and gravity, to allow the grains to mix appropriately and produce a high-density crystalline state. It is hoped that examination of the nucleation in this experiment will now enable a reliable nucleation theory, at least for this type of material.

The second analogue concerns the phase transitions, in large constrained networks, discovered in a recent series of papers joint with R. Kenyon, K. Ren and L. Sadun [4, 5]. It is tempting to use the nucleation idea to study the transition between ordered and disordered phases found in this purely mathematical setting: to study 'how' a graph typical of a disordered phase turns into one typical of a neighboring ordered phase. An ongoing project was described, joint with J. Neeman and L. Sadun, in which an appropriate random dynamics is introduced rearranging edges so as to drive the system between the phases.

The notion of Wulff shape was also discussed, appropriate for a finite but macroscopic material in a fluid or solid phase (rather than for coexisting phases, like an ice cube in water, as is often done), and was illustrated by a recent granular experiment by N. Sakai [6]. A formalism and open problems are discussed in [7].

Phase transitions in statistical mechanics have been a good source of mathematics. Nucleation theory is an associated dynamical theory. Its goal is to understand how a microstate typical of one phase transforms into a microstate typical of a neighboring phase. For materials made of molecules the theory is not in good shape, and the two regimes we discussed, bulk sand and constrained networks, provide tempting starting points for creation of a better mathematical framework.

Modeling Wulff shapes for pure phases is more advanced theoretically than the above, with a plausible framework and open problems listed in [7].

References

[1] F. Rietz, C. Radin, H. Swinney and M. Schroeter, *Nucleation in sheared granular matter*, Phys. Rev. Lett. **120** (2018) 055701.

[2] C. Radin and H. Swinney, *Phases of granular matter*, J. Stat. Phys. (2018) doi.org/10.10/s10955-018-2144-4

[3] S.F. Edwards and R.B.S. Oakeshott, *Theory of powders*, Physica A **157** (1989) 1080–1090.

[4] R. Kenyon, C. Radin, K. Ren and L. Sadun, *The phases of large networks with edge and triangle constraints*, J. Phys. A: Math. Theor. **50** (2017) 435001.

[5] C. Radin, *Phases in large combinatorial systems*, Ann. Inst. H. Poincaré D **5** (2018) 287–308.

[6] N. Sakai, S. Moulinet, F. Lechenault and M. Adda-Bedia, *Experimental evidence of thermal-like behaviour in dense granular suspensions* arXiv:1701.02209v2 (2018).

[7] C. Radin, *The open mathematics of crystallization*, Notices Amer. Math. Soc. **64** (2017) 551–556.

On the pattern formation for a family of functionals with short-range/long-range interactions in competition

Eris Runa
(joint work with Sara Daneri)

Pattern formation is an ubiquitous phenomena in nature. It can be observed both in experiments and numerical simulations. One of the most common situations in which pattern formation occurs is the competition between a short-range attractive and a long-range repulsive interaction. We will be most interested in the formation of the periodic stripes. Some specific examples where one observes the formation of periodic stripes are: colloidal systems, magnetic thin films, superconductors, diblock copolymer, twinned martesites.

One of the main difficulties is that the minimizers are invariant under a smaller group of symmetries than the functional itself (this is sometimes called symmetry breaking in the literature).

We will consider a class of functionals with short-range/long-range interactions and show that the minimizers are periodic stripes. In the continuous setting, to our knowledge our result is the first example of a model with short-range/long-range terms in competition such that the functional is invariant under permutation of coordinates and the minimizers display a pattern formation which is one-dimensional.

Although the class of functionals for which periodic stripes are the minimizers is larger, we will concentrate on the continuous case where the local term is the 1-perimeter term and the nonlocal term is based on a kernel decaying with exponent $p \geq d+2$, being d the dimension of the underlying Euclidean space.

Let us now be more precise: for $E \subset \mathbb{R}^d$, $d \geq 1$, $L > 0$

(1)
$$\mathcal{F}_{J,L}(E) = \frac{1}{L^d}\Big(J\mathrm{Per}_1(E,[0,L)^d) - \int_{[0,L)^d}\int_{\mathbb{R}^d} |\chi_E(x)-\chi_E(y)|K_1(x-y)\mathrm{d}y\mathrm{d}x\Big),$$

where J is a positive constant, Per_1 is the 1-perimeter and $|\cdot|_1$ is the 1-norm and $K_1(\zeta) := \frac{1}{(|\zeta|_1+1)^p}$.

The perimeter term acts as short-range attracting force and the long-range term as repulsive long-range force.

In order to make our problem well-posed, we restrict the functional to $[0,L)^d$-periodic sets.

Assuming initially that E is composed of stripes, by using the reflection positivity technique, one can see that there exists h_J^* such that periodic stripes of width and distance h_J^* are minimizers among sets composed of stripes.

In the following theorem, we show that periodic stripes are actually global minimizers, as soon as L is an even multiple of h_J^*.

Theorem 1. *Let $d \geq 1$, $p \geq d+2$. Then there exists τ_0, such that for every $0 < J_c - J < \tau_0$, one has that for every $k \in \mathbb{N}$ and $L = 2kh_J^*$, the minimizers of $\mathcal{F}_{J,L}$ are optimal periodic stripes.*

Some of the ingredients of the paper are: a two-scale analysis, a rigidity result and application of the reflection positivity.

References

[1] A. Giuliani and R. Seiringer. Periodic striped ground states in Ising models with competing interactions. *Comm. Math. Phys.*, 1–25, 2016.

[2] S. Daneri and E. Runa. Exact periodic stripes for minimizers of a local/non-local interaction functional in general dimension ArXiv:1702.07334, 2017.

[3] M. Goldman and E. Runa. On the optimality of stripes in a variational model with nonlocal interactions. *ArXiv:1611.07228*, 2016.

[4] L.D. Landau and E.M. Lifshitz. Course of Theoretical Physics, vol. 8. Pergamon, London, 1984.

[5] T. Ohta and K. Kawasaki. Equilibrium morphology of block copolymer melts. *Macromolecules*, 19(10):2621–2632, 1986.

[6] K. Osterwalder and R. Schrader Axioms for Euclidean Green's functions. *Comm. Math. Phys*, 31, 83-112, 1973.

[7] A. Hubert and R. Schafer. Magnetic domains: the analysis of magnetic microstructures. *Springer Science and Business Media*, 1998.

[8] M. Seul and D. Andelman. Domain shapes and patterns: The phenomenology of modulated phases. *Science*, 267(5197):476–483, 1995.

Compactness for a Γ-development for discrete systems with non-convex interaction potentials and external forces

Anja Schlömerkemper

(joint work with Marcello Carioni and Julian Fischer)

Passages from discrete to continuous systems of particles have been the subject of research with various approaches for many years. Here we focus on one-dimensional particle systems with non-convex nearest-neighbour as well as next-to-nearest neighbour interactions, which allow for the formation of cracks. The novelty is that external forces are included; these may depend on the material points or on the deformed configuration, i.e. on Lagrangian or Eulerian coordinates. Hence the forces may be related to dead as well as live loads. The interest in one-dimensional systems is three fold: they serve as toy models, avoid certain mathematical problems of higher-dimensional systems and have applications in linear atomic structures like carbon atom wires, see [1] for references and details.

Our analysis is based on methods involving Γ-convergence, which is a notion of variational convergence. As pointed out in previous works, the Γ-limit as the number of particles tends to infinity is not sufficient for describing cracks: it yields an integral functional which is the contribution from the bulk energy that does not show any information on the size of the crack. The reason for this is that the integrand of the bulk term is the convex hull of an effective energy density and consequently has infinitely many minimizers. This justifies the need for a better approximation. Here we thus consider the so-called Γ-limit of first order, which yields information on surface energies, i.e., on the energy needed during the formation of cracks.

The proof of the Γ-limit of first order requires the proof of a related compactness result, which we provide in [1]. In the presence of external forces this requires a novel method. Without external forces one compares the energy of a configuration of particles to the global minimum of the Γ-limit without external forces. Here, instead, we compare to the energy of a competitor in some subclass of functions which are in a certain sense close to the configuration. The essential novelty is the construction of such a suitable competitor and a careful analysis of their discrete gradients, see again [1].

Furthermore we provide a detailed study of the minimizers of the Γ-limit with external forces. Depending on the external force, we give a characterization of the points of the domain where a non-elastic behaviour can occur. Moreover, we study the size of a crack in relation to the external force. It turns out that the minimizers have a certain regularity and that there is no region with a complete compression.

In future work, a full proof of the Γ-limit of first order will be presented.

References

[1] M. Carioni, J. Fischer, A. Schlömerkemper, *External forces in the continuum limit of discrete systems with non-convex interaction potentials: Compactness for a Γ-development*, arXiv:1811.09857.

Variational models, partial differential equations and machine learning for mathematical imaging

Carola-Bibiane Schönlieb

Images are a rich source of beautiful mathematical formalism and analysis. Associated mathematical problems arise in functional and non-smooth analysis, variational calculus, the theory and numerical analysis of partial differential equations, harmonic, stochastic and statistical analysis, and optimisation. Starting with a discussion on the intrinsic structure of images and their mathematical representation, in this lecture we learned about variational regularisation models in mathematical imaging and their connection to partial differential equations, and went all the way to the challenges of their mathematical analysis as well as the hurdles for solving these - typically non-smooth- models computationally [16]. We presented several applications of these approaches, among others applications in image segmentation [7, 12, 6], image fusion [3, 4] and motion-estimation [11]. We also showcased some recent machine learning approaches to the solution of mathematical imaging problems. The journey took us from bilevel learning for total variation type regularisation models [8, 14, 5, 9, 10] to task-oriented learned iterative reconstruction with neural networks [13, 1, 2] and adversarial regularisers [15], with applications to image de-noising, computed tomography and Magnetic Resonance Imaging.

References

[1] J. Adler, O. Öktem, *Learned primal-dual reconstruction*, IEEE transactions on medical imaging, 37(6), 1322-1332, 2018.

[2] J. Adler, S. Lunz, O. Verdier, C.-B. Schönlieb, O. Öktem, *Task adapted reconstruction for inverse problems*, in NIPS 2018 meets medical imaging: Workshop within the 32nd annual conference on neural information processing systems (NIPS 2018). Also available as arXiv e-print: `https://arxiv.org/abs/1809.00948`.

[3] M. Benning, M. Möller, R. Z. Nossek, M. Burger, D. Cremers, G. Gilboa and C.-B. Schönlieb, *Nonlinear Spectral Image Fusion*, Scale Space Var. Meth. Comp. Vis. (SSVM), 12 p., 2017.

[4] L. Bungert, D. A. Coomes, M. J. Ehrhardt, J. Rasch, R. Reisenhofer, C.-B. Schönlieb, *Blind Image Fusion for Hyperspectral Imaging with the Directional Total Variation*, Inverse Problems, 34(4), 044003, 2018.

[5] L. Calatroni, C. Cao, J.C. De Los Reyes, C.-B. Schönlieb, T. Valkonen, *Bilevel approaches for learning of variational imaging models*, Variational Methods, 252-290, 2016.

[6] L. Calatroni, Y. van Gennip, H. Rowland, C.-B. Schönlieb, A. Flenner, *Graph clustering, variational image segmentation methods and Hough transform scale detection for object measurement in images*, J Math Imaging Vis, 57: 269, 2017.

[7] T.F. Chan, L.A. Vese, *An active contour model without edges*, Lecture Notes in Computer Science, vol. 1682, pp. 141?151, 1999.

[8] J. C. De los Reyes, C.-B. Schönlieb, *Image denoising: Learning the noise model via nonsmooth PDE-constrained optimization*, Inverse Problems & Imaging, 7(4), 1183-1214, 2013.

[9] J.C. De los Reyes, C.-B. Schönlieb, T. Valkonen, *The structure of optimal parameters for image restoration problems*, Journal of Mathematical Analysis and Applications, 434(1), 464-500, 2016.

[10] J. C. De los Reyes, C.-B. Schönlieb, T. Valkonen, *Bilevel parameter learning for higher-order total variation regularisation models*, Journal of Mathematical Imaging and Vision, 57(1), 1-25, 2017.

[11] M. Burger, H. Dirks, C.-B. Schönlieb, *A Variational Model for Joint Motion Estimation and Image Reconstruction*, SIAM J. Imaging Sci., 11(1), 94-128, 2018.

[12] J. Grah, J. Harrington, S. Boon Koh, J. Pike, A. Schreiner, M. Burger, C.-B. Schönlieb, S. Reichelt, *Mathematical Imaging Methods for Mitosis Analysis in Live-Cell Phase Contrast Microscopy*, Methods, 115, 91-99, 2017.

[13] E. Kobler, T. Klatzer, K. Hammernik, T. Pock, *Variational networks: connecting variational methods and deep learning*, In German Conference on Pattern Recognition (pp. 281-293). Springer, Cham, 2017, September.

[14] K. Kunisch, T. Pock, *A bilevel optimization approach for parameter learning in variational models*, SIAM Journal on Imaging Sciences, 6(2), 938-983, 2013.

[15] S. Lunz, O. Öktem, C.-B. Schönlieb, *Adversarial regularisers for inverse problems*, NIPS 2018. Also available on `https://arxiv.org/abs/1805.11572`.

[16] O. Scherzer (Ed.), *Handbook of mathematical methods in imaging*, Springer Science & Business Media, 2010.

Machine-learning interatomic potentials

Alexander Shapeev

(joint work with Konstantin Gubaev, Evgeny Podryabinkin, Gus L. W. Hart)

Atomistic simulations (such as molecular dynamics) is the largest consumer of supercomputing time worldwide. Atomistic simulations rely on one of the two models: very accurate and very computationally expensive quantum-mechanical models that resolve electronic structure, and empirical interatomic models that

postulate a simple functional form of interatomic interaction that is fast to compute. Application of ideas of machine learning has recently been put forward as a promising way to get the best out of these two models: accuracy of quantum mechanics and computational efficiency of the interatomic potentials.

A simplified problem to consider in the context of machine-learning potentials is the problem of interpolation of quantum-mechanical energies computed on a structured or unstructured mesh in the space of atomic configurations. For a machine-learning potential to be applicable to general systems, with thousands or millions of atoms, locality is used to reduce the dimensionality of such a regression problem. Locality is expressed through the assumption that the total energy is partitioned into a sum of contribution of small atomic neighborhoods (tens of atoms). This contribution as a function of relative positions of atoms in the neighborhood will be called the interatomic *potential*. This regression problem thus reduces to finding the best potential that reproduces the quantum-mechanical data—this is a more general (and harder) problem than a simple interpolation since the underlying quantum-mechanical potential is not given, only the total energy is. In simple settings, where the interaction strength decay exponentially in space [1], one can prove approximation bounds on such an approach to partitioning the total energy. However, beyond such simple settings, it is an open problem what is a good way to account for locality.

Imagine a neighborhood of an atom with nearest and next-nearest neighbors in a face-centered cubic lattice. This central atom has $n = 18$ neighbors and the potential V thus depends on $3n = 54$ independent parameters $\boldsymbol{u} = (u_i)_{i=1,\dots,n}$, $u_i \in \mathbb{R}^3$. This dimensionality is still large, however, as we will see, physical symmetries come to rescue. Moment Tensor Potentials (MTPs) used in the work are constructed as polynomials of atomic positions relative to the position of the central atom in an environment. The actual basis functions of atomic environments are polynomials post-processed to ensure a smooth cutoff when an atoms leaves the environment. It turns out that requiring these polynomials to be invariant with respect to rotation, reflection, and permutation invariance reduces the number of polynomial parameters drastically. For example, there are $(3n + 1)^2/2 = 1540$ monomials of degree 2 or less, but only two linearly independent polynomials are invariant, $p_1(\boldsymbol{u}) = 1$ and $p_2(\boldsymbol{u}) = \sum_{i=1}^{n} |u_i|^2$. The MTP potentials thus constructed are described in detail in [4].

A potential V is defined as a linear combination of the basis functions with coefficients found from the training set—a set of configurations whose energies, forces, and stresses are computed by a quantum-mechanical model. The problem one faces when trying to apply machine-learning potentials in practice is the lack of transferability—a potential "easily finds" configurations "far away" from the training set, on which the prediction involves some kind of extrapolation and therefore is not reliable. We are solving this problem by *active learning*, namely with a D-optimality criterion [3]. In a nutshell, we consider the vectors of our N invariant basis functions as descriptors of atomic configurations in an N-dimensional space. We impose the restriction that the training set contains N configurations

and define the quality of the training set as the volume of the simplex based on vectors corresponding to the N training configurations. We say that prediction on a new configuration involves extrapolation if, by definition, we can replace some training configuration by a new configuration such that the volume of the simplex increases. Hence, our strategy of assembling the training on the fly is to include all extrapolative configurations into the training set. This way we avoid extrapolation in practical applications.

Take the problem of construction of convex hull of thermodynamically stable alloy structures. The state-of-the-art approach consists of using thousand to few thousands of *crystal prototypes*—a set of very carefully chosen structures equilibrating which using the density functional theory (DFT) would likely yield low-energy structures on the convex hull. With the actively learning MTP, it is possible to expand the pool of candidate structures to hundred thousand configurations, equilibrate them while simultaneously learning the interatomic potential, and thus screen out all but a few thousands structures that can be equilibrated on DFT. As a result, one obtains an improved convex hull with a 100-fold speedup as compared to the scenario when all the initial structures are equilibrated with DFT [2].

References

[1] Huajie Chen and Christoph Ortner. *QM/MM methods for crystalline defects. Part 1: Locality of the tight binding model.* Multiscale Modeling & Simulation **14** (2016), 232–264.

[2] Konstantin Gubaev, Evgeny V Podryabinkin, Gus LW Hart, and Alexander V Shapeev. *Accelerating high-throughput searches for new alloys with active learning of interatomic potentials.* Computational Materials Science **156** (2019), 148–156.

[3] Evgeny V Podryabinkin and Alexander V Shapeev. *Active learning of linearly parametrized interatomic potentials.* Computational Materials Science **140** (2017), 171–180.

[4] Alexander V Shapeev. *Moment tensor potentials: A class of systematically improvable interatomic potentials.* Multiscale Modeling & Simulation **14** (2016), 1153–1173.

Variational problems of machine learning and their continuum limits

Dejan Slepčev

(joint work with Xavier Bresson, Jeff Calder, Marco Caroccia, Antonin Chambolle, Nicolás García Trillos, Moritz Gerlach, Matthias Hein, Thomas Laurent, Andrew Stuart, Matthew Thorpe, James von Brecht)

We discussed variational problems arising in machine learning and their limits as the number of data points goes to infinity. Consider point clouds obtained as random samples of an underlying "ground-truth" measure. Graph representing the point cloud is obtained by assigning weights to edges based on the distance between the points. Many machine learning tasks, such as clustering and semi-supervised learning, can be posed as minimizing functionals on such graphs [1, 13, 14, 18].

We consider functionals involving graph cuts [10, 12], graph Laplacians [4, 11], graph p-Laplacians [3, 16], higher-order graph fractional laplacians [7], Mumford-Shah functionals on graphs [5, 15] and their limits as the number of data points

goes to infinity. In particular we establish under what conditions the minimizers of discrete problems have a well defined continuum limit.

To do so we combine techniques of calculus of variations, in particular Γ-convergence [2, 6], optimal transportation [9], probability and statistics.

References

[1] M. Belkin and P. Niyogi. *Using manifold structure for partially labeled classification*, In *Advances in Neural Information Processing Systems (NIPS)*, (2003), 953–960,.

[2] A. Braides. Γ*-convergence for beginners*, volume 22 of *Oxford Lecture Series in Mathematics and its Applications*. Oxford University Press, Oxford, (2002).

[3] J. Calder. *The game theoretic p-Laplacian and semi-supervised learning with few labels*, *arXiv:1711.10144*, (2017).

[4] J. Calder, and D. Slepčev *Properly-weighted graph Laplacian for semi-supervised learning*, *arXiv:1810.04351*, (2018).

[5] M. Caroccia, A. Chambolle, D. Slepčev, *Mumford – Shah functionals on graphs and their asymptotics*, in preparation, (2018).

[6] G. Dal Maso. *An introduction to* Γ*-convergence*, *Progress in Nonlinear Differential Equations and their Applications*. Birkhäuser Boston, Inc., Boston, MA, **8** (1993).

[7] M. M. Dunlop, D. Slepčev, A. M. Stuart, and M. Thorpe. *Large data and zero noise limits of graph-based semi-supervised learning algorithms*, arXiv:1805.09450, (2018).

[8] N. García Trillos, M. Gerlach, M. Hein, and D. Slepčev. *Error estimates for spectral convergence of the graph Laplacian on random geometric graphs towards the Laplace-Beltrami operator*, arXiv:1801.10108, (2018).

[9] N. García Trillos and D. Slepčev. *On the rate of convergence of empirical measures in* ∞*-transportation distance*, *Canad. J. Math.*, **67** (2015), 1358–1383.

[10] N. García Trillos and D. Slepčev. *Continuum limit of total variation on point clouds*, *Archive for Rational Mechanics and Analysis*, **220** (2016), 193–241.

[11] N. García Trillos and D. Slepčev. *A variational approach to the consistency of spectral clustering*, *Appl. Comput. Harmon. Anal.*, **45** (2018), 239–281.

[12] N. García Trillos, D. Slepčev, J. von Brecht, T. Laurent, and X. Bresson. *Consistency of Cheeger and ratio graph cuts*, *J. Mach. Learn. Res.*, **17** (2016), 1-46.

[13] R. Kannan, S. Vempala, and A. Vetta. *On clusterings: Good, bad and spectral*, *Journal of the ACM (JACM)*, **51** (2004), 497–515.

[14] A. Y. Ng, M. I. Jordan, and Y. Weiss, *On spectral clustering: Analysis and an algorithm*, in Advances in Neural Information Processing Systems (NIPS), MIT Press, (2001), 849–856.

[15] M. Ruf. *Discrete stochastic approximations of the Mumford-Shah functional*, arXiv:1710.05571, (2017).

[16] D. Slepčev and M. Thorpe. *Analysis of p-Laplacian regularization in semi-supervised learning*, *arXiv:1707.06213*, (2017).

[von Luxburg(2007)] U. von Luxburg. *A tutorial on spectral clustering*, *Statistics and Computing*, **17** (2007), 395–416.

[17] X. Zhou and M. Belkin. *Semi-supervised learning by higher order regularization*, In *Proceedings of the 14th International Conference on Artificial Intelligence and Statistics*, *Proceedings of Machine Learning Research*, **15** (2011), 892–900.

[18] X. Zhu, Z. Ghahramani, and J. Lafferty, *Semi-supervised learning using Gaussian fields and harmonic functions*, In *International Conference on Machine Learning*, **3** (2003), 912–919.

Discrete-to-Continuum Limits of p-Laplacian Regularisation in Semi-Supervised Learning on Graphs

Matthew Thorpe
(joint work with Dejan Slepčev)

The talk concerns how a family of regression problems in a semi-supervised setting behaves in the large data limit. The task is to assign real-valued labels to a set $X_n = \{x_i\}_{i=1}^n \subset \mathbb{R}^d$ of n sample points, provided a small training subset of N labelled points, i.e. we are given labels $\{y_i\}_{i=1}^N$ on the first N data points.. We pose the problem on a graph $G = (X_n, W)$ where X_n form the nodes of the graph and $W = (W_{ij})_{i,j=1}^n$ are edge weights. More precisely, we use random geometric graphs where one defines a connectivity radius ε and weights by

$$W_{ij} = \eta_\varepsilon(|x_i - x_j|) = \frac{1}{\varepsilon^d}\eta\left(\frac{|x_i - x_j|}{\varepsilon}\right).$$

A prototypical example is $\eta(t) = 1$ if $|t| \leq 1$ and $\eta(t) = 0$ for $|t| > 1$, so that the graph has positive weights only when nodes are closer than ε. In order to localise the geometry we choose $\varepsilon = \varepsilon_n$ and let $\varepsilon_n \to 0$ as $n \to \infty$.

We use an objective functionals which rewards the regularity of the estimator function and imposes agreement with the training data. In particular, we consider discrete p-Laplacian regularization defined by

$$\mathcal{E}_n^{(p)}(f) = \frac{1}{\varepsilon_n^p n^2}\sum_{i,j=1}^n W_{ij}|f(x_i) - f(x_j)|^p.$$

The variational problem we consider is

$$\text{minimise } \mathcal{E}_n^{(p)}(f) \text{ subject to } f(x_i) = y_i \text{ for all } i = 1, \dots, N.$$

If data points x_i are independently sampled from a probability measure $\mu \in \mathcal{P}(\mathbb{R}^d)$ with density ρ then a formal argument shows that the pointwise limit of $\mathcal{E}_n^{(p)}$ is

$$\mathcal{E}_\infty^{(p)}(f) = \sigma\int_{\mathbb{R}^d} |\nabla f(x)|^p \rho^2(x)\,\mathrm{d}x$$

with probability one. In the $n \to \infty$ the choice of η in the weights is present only through the constant σ (at least for isotropic weights).

The question we ask is whether the constrained minimisers of $\mathcal{E}_n^{(p)}$ converge to constrained minimisers of $\mathcal{E}_\infty^{(p)}$ as $n \to \infty$ for N fixed. Clearly the constrained limiting problem only makes sense for $p > d$. It is natural to ask whether this is sufficient. As it turns out one needs to control the length scale ε_n. We uncover a delicate interplay between the regularizing nature of the functionals considered and the nonlocality inherent to the graph constructions. Our main result is that constrained minimisers of $\mathcal{E}_n^{(p)}$ converge to constrained minimisers of $\mathcal{E}_\infty^{(p)}$ when

$$\varepsilon_n^p n \to 0$$

(the well posed regime) and when

$$\varepsilon_n^p n \to \infty$$

constrained minimisers converge to constants (ill posed regime). The condition $\varepsilon_n^p n \to 0$ implies an upper bound on ε_n. We introduce a new model which is as simple as the original model, but overcomes this restriction.

The proof uses methods from the calculus of variations, namely Γ-convergence, coupled with an optimal transport based metric where one can define the discrete-to-continuum topology necessary to define a notion of convergence for functions on the graph. Precise statements and proofs can be found in [1].

References

[1] D. Slepčev and M. Thorpe, *Analysis of p-Laplacian Regularization in Semi-Supervised Learning*, arXiv:1707.06213 (2017).

On asymptotic gradient flow structures of PDE models with excluded volume effects

Marie-Therese Wolfram

(joint work with Maria Bruna, Martin Burger and Helene Ranetbauer)

Cross diffusion systems arise naturally in the context of interacting multi-species systems. These models have been used to describe bidirectional flows of pedestrians, differently charged particles in nanoscale pores or the motion of colloid particles in suspensions. In all these applications the physical size of the particles plays an important role in the dynamics and should be accounted for in the mean-field limit. However in the presence of finite volume effects, the limiting passage from the micro- to the macroscopic systems is still an open question. Different mean-field systems were formally derived - they do have a different structure, but all of them have cross diffusion terms. In addition they often lack a full gradient flow (GF) structure (even though the microscopic system had a natural gradient flow structure). The lack of such is caused by approximations made in the derivation, however the systems often agree with a GF up to a certain order of expansion. We refer to such systems asymptotic gradient flow (AGF) in the following.
In this talk we discuss the notion of AGF for a cross diffusion system, which was derived by Bruna and Chapman in [1] from a stochastic system of interacting Brownian particles using the method of matched asymptotics. The system has a GF structure in the symmetric case of all particles having the same size and diffusivity and an AGF structure in general. However the 'closeness' of the AGF to a full GF can be used to study the behaviour of solution near the equilibrium. In the special case of one species being stationary, the system reduces to a nonlinear Fokker-Planck equation. This scalar equation has again an AGF structure. We discuss its possible entropy-mobility pairs and compare their respective equilibrium solutions with the stationary solution of the AGF and MC simulations of the underlying particle system. Depending on the parameter regime considered, the

different entropies match better or worse with the MC simulations. Apart from their approximation quality, these entropies provide different a-priori estimates. We discuss their advantages and disadvantages from the analytic perspective and show how they can be used in different global in time existence results for the respective AGF and GF structures.

References

[1] M. Bruna and S. J. Chapman,*Diffusion of multiple species with excluded-volume effects*, J. Chem. Phys., **137**(2012), pp. 204116-204116-16.

[2] M. Bruna, M. Burger, H. Ranetbauer, M.T. Wolfram, *Cross-diffusion systems with excluded volume effects and asymptotic gradient flows*, Journal of Nonlinear Science **27**(2016).

[3] M.Bruna, M. Burger, H. Ranetbauer, M.T. Wolfram, *Asymptotic gradient flow structures of a nonlinear Fokker Planck equation*, Arxiv arXiv preprint arXiv:1708.07304, submitted, 2018

Reporter: David Melching

Participants

Prof. Dr. Stefan Adams
Mathematics Institute
University of Warwick
Zeeman Building
Coventry CV4 7AL
UNITED KINGDOM

Prof. Dr. Roberto Alicandro
D.I.E.I.
Università di Cassino
Via di Biasio, 43
03043 Cassino (FR)
ITALY

Prof. Dr. Michael Baake
Fakultät für Mathematik
Universität Bielefeld
Postfach 100131
33501 Bielefeld
GERMANY

Dr. Annika Bach
Zentrum Mathematik - M 7
Technische Universität München
Boltzmannstraße 3
85748 Garching bei München
GERMANY

Dr. Laurent Bétermin
Institut for Matematiske Fag
Kobenhavns Universitet
Universitetsparken 5
2100 København
DENMARK

Prof. Andrea Braides
Dipartimento di Matematica
Universita di Roma "Tor Vergata"
via della Ricerca Scientifica, 1
00133 Roma
ITALY

Dr. Julian Braun
Mathematics Institute
University of Warwick
Zeeman Building
Coventry CV4 7AL
UNITED KINGDOM

Dr. Marco Caroccia
Department of Mathematical Sciences
Carnegie Mellon University
Pittsburgh, PA 15213-3890
UNITED STATES

Prof. Dr. Paolo Cermelli
Dipartimento di Matematica
Universita degli Studi di Torino
Via Carlo Alberto, 10
10123 Torino
ITALY

Prof. Dr. Marco Cicalese
Zentrum Mathematik - M 7
Technische Universität München
Boltzmannstraße 3
85748 Garching bei München
GERMANY

Dr. Elisa Davoli
Fakultät für Mathematik
Universität Wien
Oskar-Morgenstern-Platz 1
1090 Wien
AUSTRIA

Dr. Lucia De Luca
SISSA
International School for Advanced Studies
Via Bonomea 265
34136 Trieste
ITALY

Prof. Dr. Patrick W. Dondl
Abteilung für Angewandte Mathematik
Universität Freiburg
Hermann-Herder-Strasse 10
79104 Freiburg i. Br.
GERMANY

Simone Dovetta
DISMA
Politecnico di Torino
Corso Duca degli Abruzzi, 24
10129 Torino
ITALY

Prof. Dr. Manuel Friedrich
Institut für Angewandte Mathematik
Universität Münster
Einsteinstrasse 62
48149 Münster
GERMANY

Prof. Dr. Maria Stella Gelli
Dipartimento di Matematica "L.Tonelli"
Universita di Pisa
Largo Bruno Pontecorvo, 5
56127 Pisa
ITALY

Prof. Dr. Peter J. Grabner
Institut für Analysis und Zahlentheorie
Technische Universität Graz
Kopernikusgasse 24/II
8010 Graz
AUSTRIA

Prof. Dr. Markus Heydenreich
Mathematisches Institut
Ludwig-Maximilians-Universität München
Theresienstrasse 39
80333 München
GERMANY

Dr. Martin Jesenko
Mathematisches Institut
Universität Freiburg
Hermann-Herder-Strasse 10
79104 Freiburg i. Br.
GERMANY

Dr. Sebastian Kapfer
Institut für Theoretische Physik I
FAU Erlangen-Nürnberg
Staudtstrasse 7
91058 Erlangen
GERMANY

Dr. Leonard Kreutz
Institut für Angewandte Mathematik
Universität Münster
Einsteinstrasse 62
48149 Münster
GERMANY

Prof. Dr. Stephan Luckhaus
Mathematisches Institut
Universität Leipzig
Postfach 10 09 20
04109 Leipzig
GERMANY

Prof. Dr. Mitchell B. Luskin
School of Mathematics
University of Minnesota
127 Vincent Hall
206 Church Street S. E.
Minneapolis MN 55455-0436
UNITED STATES

Dr. Edoardo Mainini
Dipartimento di Matematica
Universita di Genova
Via Dodecaneso 35
16146 Genova
ITALY

David Melching
Fakultät für Mathematik
Universität Wien
Oskar-Morgenstern-Platz 1
1090 Wien
AUSTRIA

Dr. Sara Merino-Aceituno
Fakultät für Mathematik
Universität Wien
Oskar-Morgenstern-Platz 1
1090 Wien
AUSTRIA

Prof. Dr. Franz Merkl
Mathematisches Institut
Ludwig-Maximilians-Universität
München
Theresienstrasse 39
80333 München
GERMANY

Prof. Dr. Maria Giovanna Mora
Dipartimento di Matematica
Università di Pavia
Via Ferrata, 1
27100 Pavia
ITALY

Prof. Dr. Michael Ortiz
Division of Engineering and
Applied Sciences, MS 104-44
California Institute of Technology
Pasadena, CA 91125
UNITED STATES

Prof. Dr. Mark A. Peletier
Department of Mathematics
Eindhoven University of Technology
P.O.Box 513
5600 MB Eindhoven
NETHERLANDS

Dr. Paolo Piovano
Fakultät für Mathematik
Universität Wien
Oskar-Morgenstern-Platz 1
1090 Wien
AUSTRIA

Dr. Marcello Ponsiglione
Dipartimento di Matematica
Universita di Roma "La Sapienza"
Istituto "Guido Castelnuovo"
Piazzale Aldo Moro, 2
00185 Roma
ITALY

Prof. Dr. Charles Radin
Department of Mathematics
The University of Texas at Austin
1 University Station C1200
Austin, TX 78712-1082
UNITED STATES

Dr. Eris Runa
Max-Planck-Institut für Mathematik
in den Naturwissenschaften
Inselstrasse 22 - 26
04103 Leipzig
GERMANY

Dr. Lucia Scardia
Department of Mathematics
Heriot-Watt University
Riccarton
Edinburgh EH14 4AS
UNITED KINGDOM

William Schill
Graduate Aeronautical Laboratories
California Institute of Technology
MS 105-50
Pasadena, CA 91125
UNITED STATES

Prof. Dr. Anja Schlömerkemper
Institut für Mathematik
Universität Würzburg
Emil-Fischer-Straße 40
97074 Würzburg
GERMANY

Prof. Dr. Bernd Schmidt
Institut für Mathematik
Universität Augsburg
86135 Augsburg
GERMANY

Prof. Dr. Carola-Bibiane Schönlieb
Department of Applied Mathematics and Theoretical Physics (DAMTP)
Centre for Mathematical Sciences
Wilberforce Road
Cambridge CB3 0WA
UNITED KINGDOM

Prof. Dr. Alexander V. Shapeev
Center for Advanced Studies
Skolkovo Institute of Science and Technology
1 Nobel Street
Moscow 143 026
RUSSIAN FEDERATION

Prof. Dr. Dejan Slepcev
Department of Mathematical Sciences
Carnegie Mellon University
5000 Forbes Avenue
Pittsburgh, PA 15213-3890
UNITED STATES

Prof. Dr. Margherita Solci
DADU
Università di Sassari
Palazzo del Pou Salit
Piazza Duomo, 6
07041 Alghero
ITALY

Prof. Dr. Ulisse Stefanelli
Fakultät für Mathematik
Universität Wien
Oskar-Morgenstern-Platz 1
1090 Wien
AUSTRIA

Martin G. Steinbach
Institut für Mathematik
Universität Augsburg
86135 Augsburg
GERMANY

Prof. Dr. Florian Theil
Mathematics Institute
Warwick University
Zeeman Building
Coventry CV4 7AL
UNITED KINGDOM

Dr. Matthew Thorpe
Department of Applied Mathematics and Theoretical Physics (DAMTP)
Centre for Mathematical Sciences
Wilberforce Road
Cambridge CB3 0WA
UNITED KINGDOM

Antonio Tribuzio
Dipartimento di Matematica
Universita degli Studi di Roma II
"Tor Vergata"
via della Ricerca Scientifica, 1
00133 Roma
ITALY

Dr. Marie-Therese Wolfram
Mathematics Institute
University of Warwick
Zeeman Building
Coventry CV4 7AL
UNITED KINGDOM

Prof. Dr. Caterina Zeppieri
Institut für Angewandte Mathematik
Universität Münster
Einsteinstrasse 62
48149 Münster
GERMANY

Prof. Dr. Barbara Zwicknagl
Institut für Mathematik
Sekr. MA 6-4
Technische Universität Berlin
Straße des 17. Juni 136
10623 Berlin
GERMANY